THE INFLUENCE OF HDAC INHIBITION ON THE MAINTAINANCE OF IRON HOMEOSTASIS AND THE ACQUISITION OF ONCOGENIC PHENOTYPES IN CANCER CELLS

By

THAIS GAIA OLIVEIRA

Bachelor of Science in Nutrition and Dietetics

East Carolina University

Greenville, North Carolina

2019

Submitted to the Faculty of the
Graduate College of the
Oklahoma State University
in partial fulfillment of
the requirements for
the Degree of
MASTER OF SCIENCE
May, 2021

THE INFLUENCE OF HDAC INHIBITION ON THE

MAINTAINANCE OF IRON HOMEOSTASIS

AND THE ACQUISITION OF ONCOGENIC

PHENOTYPES IN CANCER CELLS

Thesis Approved:

Dr. Mckale Montgomery

Thesis Adviser

Dr. Winyoo Chowanadisai

Dr. Daniel Lin

ACKNOWLEDGEMENTS

There are many out there would need to give acknowledgements to, but let's keep it short and sweet. First of all, I am thankful for being given the opportunity to work on this research by Dr. Mckale Montgomery. I'm grateful for being the one she chose to take over this project. I learned a lot from her – attention to details, detailed record keeping, proper pipetting, scientific writing, thought process, and many other skills that I carry with me to the rest of my life. In addition, you can learn a lot by just observing, she leads by example for sure. In fact, people around here have noticed my organization and attention to details, and praised me for it, and I have this lab to be thankful for. I also have Evan Herman to acknowledge. A great lab mate, he is patient (sometimes too patient) and kind, he will always try to help no matter who you are or whether it is lab related or not. If somebody ever read this session and work with him, do not take him for granted, you don't find many nice people around like him. I have others to be thankful that helped to keep my sanity: Dr. Joyce, Laurie Thompson, and Ms. Mary. Laurie has thought me more than just lab skills, she has thought me about empathy (to some level), and how to keep a good humor on the face of adversity. Ah! Also, no thanks to Sanmi Alake :) There are many other people I'm thankful for and should acknowledge, but sometimes I'm a lazy Panda. Finally, I would like to acknowledge the fact of this Nutrition Science department being such a unit; here, we collaborate, and always try to help each other. This is really a unique lab, and more people should adopt this style of collaboration and caring for each other's well-being.

"Acknowledgements reflects the view of the author and are not endorsed by the committee members or Oklahoma State University"

Name: THAIS GAIA OLIVEIRA

Date of Degree: DECEMBER, 2021

Title of Study: THE INFLUENCE OF HDAC INHIBITION ON THE MAINTANANCE OF IRON HOMEOSTASIS AND THE ACQUISITION OF ONCOGENIC PHENOTYPE IN CANCER CELLS.

Major Field: NUTRITION SCIENCE

Abstract: Epithelial-to-mesenchymal transition (EMT), an essential mechanism for development and wound healing, but in cancer it also mediates the progression and spread of aggressive tumors while increasing therapeutic resistance. The use of histone deacetylase (HDAC) inhibitors as therapy is FDA approved for so-called "liquid" cancers, however, treatment success in solid tumors is limited. Although HDAC inhibitors treatment decreases proliferation, it has also been shown to induce EMT in many types of cancer cells. Adoption of a mesenchymal state is also associated with increased iron uptake, but the relationship between EMT and the key regulators of cellular iron metabolism remains undefined. In this regard, the human adrenal cortical carcinoma SW13 cell line represents an invaluable research model as it can exist as two phenotypically distinct, epithelial- (SW13-) and mesenchymal-like (SW13+) subtypes. In this study we establish SW13 cells as a model for exploring the link between iron and EMT. We then go on to show that increased iron accumulation following HDAC inhibitor-mediated EMT is associated with decreased expression of the iron export protein ferroportin, enhanced ROS production, and reduced expression of antioxidant response genes. As availability of redox active iron and loss of lipid peroxide repair capacity are hallmarks of ferroptosis, a form of iron-mediated cell death, we next examined whether HDAC inhibitor treatment could augment ferroptosis sensitivity. Indeed, HDAC inhibitor treatment synergistically increased erastin-mediated ferroptotic cell death. As several HDAC inhibitors are already FDA-approved for the treatment of certain cancer types, the findings from these studies could have immediate implications for improving iron-targeted chemotherapeutic strategies.

TABLE OF CONTENTS

Chapter Page

I. INTRODUCTION 1

II. REVIEW OF LITERATURE 4

Iron's role in the body 4
Iron uptake, utilization, and storage 5
Iron-sulfur cluster biogenesis 6
Control of cellular iron homeostasis 9
Iron regulatory proteins 9
Iron metabolism in cancer cells 10
Epithelial-to-mesenchymal transition 12
Ferroptosis: An iron mediated form of cell death 15
The epigenetic plastic SW13 cells: A model for EMT 16
Connecting the dots: HDAC inhibitor, EMT, iron, and ferroptosis 17

III. METHODOLOGY 19

Cell culture 19
Cell treatment 19
Western blot 21
Immunofluorescence 22
CellRox 22
Cell viability 23
Cell proliferation assay 23
Intracellular iron measurements 24
RNA extraction 24
Real time quantitative polymerase chain reaction 26
Electrophoretic mobility shift assay (EMSA) 27
Statistical Analyses 27

Chapter Page

IV. FINDINGS.....29

HDAC inhibitor treatment induces EMT and promotes iron accumulation in SW13 cells 29
Iron availability does not interfere with SW13 cell phenotype conversion.....32
Iron regulatory proteins contribute to iron accumulation during HDAC inhibitor-mediated SW13 cell EMT 34
Iron chelation and iron supplementation can reduce proliferation and promote cell death in HDAC inhibitor treated SW13 cells 36
SW13 cells exhibit oxidative stress during HDAC inhibitor mediated EMT.....38
HDAC inhibition enhances ferroptosis sensitivity in mesenchymal-like SW13 cells 40

V. Discussion 42

VI. Conclusion 47

REFERENCES 50

LIST OF TABLES

Table Page

1 A summary of iron regulatory elements (IREs) containing mRNAs.....8
2 Prime sequences for qPCR.....26

LIST OF FIGURES

Figure Page

1 Genes commonly expressed in the epithelial-to-mesenchymal transition 13
2 Working model for the influence of HDAC inhibitor on EMT 18
3 Illustration of the treatment timeline.....20
4 HDAC inhibitor induced SW13 phenotype conversion can serve as a model of the epithelial to mesenchymal transition 32
5 Changes in cellular iron availability does not alter HDAC inhibitor mediated EMT in SW13 cells 33
6 IRP mRNA binding activity is increased and ferroportin expression is decreased following HDAC inhibitor0mediated EMT in SW13 cells 35
7 Both iron chelation and iron supplementation reduce cell viability in HDAC inhibitor treated SW13 cells.....37
8 HDAC inhibitor-converted mesenchymal-like SW13 cells have increased levels of ROS and reduced expression of antioxidant defense genes.....39
9 Ferroptosis induction synergistically improve HDAC inhibitor treatment on SW13 cells 41

CHAPTER I

INTRODUCTION

Iron is a trace mineral with a long, established importance with regards to its function in hemoglobin and the incidence of anemia. As advances in technology yield great breakthroughs in science, the term "trace mineral" almost demeans the vital role of iron in numerous life-preserving processes. Besides it well known role as oxygen carrier, iron is involved in many other important functions such as DNA synthesis and mitochondrial respiration. However, iron also takes part in free radical generating reactions that can cause DNA damage and significant biologic injury. It is this duplicitous nature of iron that enables it to affect both tumor initiation and growth[1-3]. Thus, iron can be therapeutically targeted for both cancer treatment and prevention. Targeting iron in cancer cells is complicated however, because the pathways that dictate cancer progression and iron utilization are regulated at multiple levels by both genetic and epigenetic means. Therefore, a better understanding of iron usage by cancer cells could assist in the development of more effective iron-targeted chemotherapies.

The two primary drivers of carcinogenesis are genetic mutations and epigenetic alterations. Genetic mutations results when changes in the nucleotide sequence such as deletion, insertion, inversion, or substitution occur in the genome, while epigenetic alterations are caused by DNA sequence-independent modifications that influence chromatin structure, such as DNA

methylation and histone modifications[4,5]. Regardless of the route, the outcome is either loss or gain of function of genes that have an influence on tumor suppression or oncogenesis, respectively.

The epithelial-to-mesenchymal-transition (EMT) is a fundamental transcriptional program that is critical for proper embryogenesis and wound healing, but that can also become aberrantly activated during pathologic conditions such as cancer, ischemia, and chronic inflammation[6-8]. During EMT, epithelial cells undergo changes in gene expression resulting in the reorganization of the cytoskeleton, changes in cell shape, and the acquisition of migratory and invasive properties as they transition to a mesenchymal state. Recent studies in the cancer biology field have identified iron as an important regulator of the EMT process by demonstrating that mesenchymal-like cancer stem cells have an increased dependence on intracellular iron[9-11]. Yet, the mechanisms promoting mesenchymal cell iron acquisition and utilization are not understood.

Ferroptosis is an iron-dependent form of programmed cell death that is impacted by biological processes such as nutrient metabolism and EMT. As mentioned above, while EMT is critical for processes such as embryogenesis and wound healing, adoption of a mesenchymal state is also associated with cancer progression, and has been implicated in renal, cardiovascular, and reproductive disorders[8,11]. Intriguingly, adoption of a mesenchymal state is associated with increased sensitivity to ferroptosis[12]. Thus, understanding the mechanisms by which adoption of a mesenchymal state contributes to increased ferroptosis sensitivity could have vast therapeutic implications.

In this regard, the human adrenal cortical carcinoma SW13 cell line represents an invaluable research model as it can exist as two phenotypically distinct, epithelial- (SW13-) and mesenchymal-like (SW13+) subtypes. Moreover, as SW13- to SW13+ subtype transition can be triggered by HDAC inhibition[13,14]. This cell culture model allows us to temporally control EMT initiation so that alterations in cellular iron metabolism can be examined during both EMT initiation and progression. The primary objective of this work was to determine how EMT influences iron homeostasis in SW13 cells. The central hypothesis was that reduced rates of cell growth and increased dependence on intracellular iron would lead to an iron regulatory signature that promotes cellular iron uptake.

CHAPTER II

REVIEW OF LITERATURE

Iron's role in the body:

Iron is an essential micronutrient that plays a vital role in many life preserving processes. For example, iron in hemoglobin is responsible for the transport, transitional tissue storage, and cellular use of oxygen. Within the mitochondria, iron has an important role in cytochromes which are responsible for electron transfer and, eventually, energy production. Cytochrome P450 is an iron containing enzyme in the liver and intestine that degrades environmental toxins and endogenous compounds. Iron is also part of heme containing enzymes such catalases that are responsible catalyzing the decomposition of hydrogen peroxide to water and oxygen; NADH dehydrogenase which is involved in the energy production; and aconitase which catalyzes the isomerization of citrate to isocitrate. Despite iron's many important roles within the body however, it is highly reactive and can create free radicals through Fenton reactions. These free radicals can cause serious damage to the cell and further biological issues such as cancer initiation and promotion[3,15-17].

Iron uptake, utilization, and storage:

Systemic iron homeostasis is regulated at the level of absorption. The duodenum is the primary site for iron absorption from the diet to the circulatory system where about 1-2 mg is absorbed through endothelial cells [18-20]. Iron is obtained from the diet as either heme or non-heme Iron. Heme iron is present in animal sources incorporated within the myoglobin and hemoglobin. Non-heme iron is found in plant-based food sources on its elemental form (Fe^{2+} or Fe^{3+}). The enterocytes are capable of only absorbing ferrous iron thus elemental iron in the ferric state must be reduced by cytochrome b at the apical membrane of duodenal enterocytes prior absorption[21]. Non-heme ferrous iron is then absorbed at the brush border via divalent metal transporter 1 (DMT1)[18]. Heme iron is carried into the enterocyte through a, as yet unidentified transporter.

Once in the enterocyte, iron can either be used to synthesize iron-containing proteins, stored in ferritin, excreted via the sloughing of enterocytes during regular intestinal cell turnover, or exported out into circulation for delivery to various tissues. Iron is exported out of enterocytes by ferroportin (SLC40A1) and oxidized by hephaestin before being picked up by transferrin (TF) for systemic distribution[22]. Once oxidized, ferrous iron is then transported systemically by TF. The expression of ferroportin is regulated by a hormonal peptide excreted by the hepatocytes, hepcidin. Under iron excess, hepcidin binds to ferroportin and causes it to be internalized and target for degradation, thereby preventing the release of iron into circulation. Under iron deficiency, the hepcidin synthesis by hepatocytes is decreased, ferroportin expression is stabilized and circulating iron levels are increased.

Transferrin receptor 1 (TFRC) is a broadly expressed receptor which is used to deliver TF bound iron into the cell. The TF/TFRC complex is internalized via endocytosis, and iron is released from the complex in the acidic environment in the endocytic vesicles[3]. Free ferrous iron is reduced by the epithelial antigen of prostate 3 (STEAP3) and exported from the endosomal membrane via DMT1 to the cytosolic labile Iron pool (LIP)[3,23]. Once inside the cell iron that is not stored or exported is used for the synthesis of iron containing proteins, synthesis of iron-sulfur clusters, and hemoglobin synthesis[18].

Ferritin is a protein responsible for safely storing iron on its non-reactive ferric state[24]. Ferritin is a spherical molecule composed of 24 subunits with a mixture of ferritin heavy chain (FTH), ~21 kDa, and ferritin light chain (FTL), ~19 kDa.[25,26]. The ratio of FTL and FHC are extremely homologous, and its ratio varies depending on cell type and in response to stimuli such as inflammation[18,24]. FTH is capable of oxidizing ferrous iron for storage while FTL facilitates iron nucleation[18]. Homologous to the cytosolic ferritin an H-type ferritin is present in the mitochondria, and it has the same function of protecting the organelle from iron's toxicity. Different from its cytosolic counterpart, mitochondrial ferritin (FtMt) is not ubiquitously expressed; it has been detected in tissues such as heart, pancreas, kidney, but not in spleen, gut or liver[18]. Finally, another major difference is that FtMt is not directly regulated by iron regulatory proteins.

Iron-sulfur cluster biogenesis:

Once inside the cell, iron is readily available for usage or storage. Iron is used to synthesize proteins, cofactors and enzymes. Among them, iron sulfur (Fe-S) clusters, are very

important cofactors that are among the most structurally and functionally versatile across all kingdoms of life [27]. Fe-S clusters are highly evolutionarily conserved, and are ubiquitous in nature, and it may be synthesized in both mitochondria or cytosol[28].

The iron sulfur cluster assembly (ISCA) machinery within the mitochondria is considered the major Fe-S cluster assembly system in humans[27]. Fe-S cluster fabrication can be divided in three main parts: cluster assembly, release of the cluster, and cluster transfer to target apo-proteins. First, the mitochondria imports iron via the mammalian carrier protein mitoferrin 1 or 2. Imported iron is then transferred to the iron sulfur scaffold assembly enzyme (ISCU) through an iron donor frataxin (FXN) and an electron donor protein ferredoxin[27,29]. Next, the cluster is released from ISCU via a chaperone system that binds to the ISCU and induces a conformational change which enables release of the cluster to Fe-S cluster carriers or specific Fe-S cluster proteins. The ABCB7 is an ATP-binding cassette (ABC) transporter located on the inner membrane of mitochondria, and it seems to be responsible for the export of Fe-S cluster and its machinery components to the cytosol[30].

The importance of Fe-S biogenesis to life is illustrated by the fact that defects in Fe-S assembly pathway can be lethal. For instance, Friedreich's ataxia, a fatal neurodegenerative disease, in which depletion of FXN causes loss of activity of Fe-S dependent enzymes. In addition, the intracellular depletion of FXN causes loss of activity of Fe-S dependent enzymes in the cytosol, mitochondria, and possibly nucleus. As a result, loss of FXN causes increased oxidative stress and iron accumulation in the mitochondria [29].

Iron regulatory elements (IREs) containing mRNAs					
mRNAs containing 5′ IREs			**mRNAs containing 3′ IREs**		
Gene Symbol	**Name**	**Function**	**Gene Symbol**	**Name**	**Function**
FTH	Ferritin H	Iron Storage	TFR1	Transferrin receptor	Iron uptake
FTL	Ferritin L	Iron Storage	DMT1	Divalent Metal transporter	Iron uptake
FPN	Ferroportin	Iron export	CDC14A	Cell division cycle 14A	Dephosphorylation of p53
HIF-2α	Hypoxia inducible factor	Hypoxia-inducible transcription factor-2α	CDC42 (MRCKα)	Cell division cycle 42	Cytoskeletal dynamics
eALAS	Erythroid aminolevulinate synthase	Heme biosynthesis	HAO1	Hydroxyacid oxidase 1	Peroxisomal enzyme
ACO2	Mitochondrial aconitase	TCA cycle; energy production			
APP	Amyloid beta precursor protein	Alzheimer's disease			

Table 1. A summary of Iron regulatory elements (IREs) containing mRNAs. Note that the 5' untranslated region containing IREs results in translational repression upon IRP/IRE binding. Conversely, IRP/IRE binding at the 3' untranslated region containing IREs stabilizes the mRNA and results in translational activation[19,20].

Control of cellular iron homeostasis:

Excluding obligatory losses through bleeding (e.g. menstruation) and the shedding of epithelial cells, there is no regulated mechanism for iron excretion, and thus iron homeostasis is tightly regulated[31]. Cellular iron homeostasis is maintained by the interaction between iron regulatory protein 1 and 2 (IRP1 and IRP2) and iron responsive elements (IREs). IRPs post-transcriptionally regulate iron homeostasis by coordinating the expression of proteins controlling cellular iron uptake, utilization, storage, and export. IREs are 26-30 nucleotide long stem-loop structures with a hairpin-like sequence of -CAGUGN- at the apical portion of the loop[32]. IREs are present in either untranslated regions of diverse mRNAs; for instance, H-ferritin, ferroportin, and m-aconitase contain single IRE at the 5' end of its mRNA while TFRC and DMT1 contain multiple IREs at the 3' end of its mRNA[20]. Under iron depleted conditions, IRP1/2 bind to the 5' end of H-ferritin which leads to repressed translation of ferritin; on the other hand, IRP-IRE binding at the 3' end of transferrin results in the stabilization of mRNA and promotes translation. As a result, iron storages decrease, and iron uptake increases. Interesting, IREs are present in several genes in which some might not even be directly related to iron metabolism as shown on table1.

Iron regulatory proteins:

Despite their similar roles in maintaining cellular iron homeostasis, IRP1 and IRP2 are differentially regulated in response to changes in iron availability[18]. IRP1 is a bifunctional protein whose behavior is dictated by either the presence or absence of an [4Fe-4S] cluster. In the presence of iron, insertion of the [4Fe-4S] cluster prevents its RNA binding activity, and IRP1

assumes its cytosolic aconitase form (holo-IRP1)[18]. In the absence of iron, the [4Fe-4S] cluster is disassembled, conferring IRP1 RNA binding and its function as a post transcriptional regulator of RNAs containing IREs (e.g. ferritin, TFRC, etc.)[33].

Independently of iron, factors that can influence biosynthesis, or stability of the [4Fe-4S] cluster can also directly impact IRP1 function. The [4Fe-4S] aconitase's cluster is solvent accessible and ROS and reactive nitrogen species (RNS) can initiate cluster loss[34]. A large number of studies demonstrated that NO and its reactive product $ONOO^-$ can facilitate the aconitase's [4Fe-4S] cluster release thus converting holo-IRP1 to apo-IRP1[35]. As a result, apo-IRP1 promotes TFR1 mRNA stabilization and translational inhibition of mRNA containing 5' IREs, such as H-ferritin and ferroportin[36,37].

Different from IRP1, IRP2 does not contains an Fe-S cluster and it function only as an RNA binding protein. Instead, IRP2 is mainly regulated at the level of protein stability by E3 ubiquitin ligase complex, SKIP1-CUL1-FBXL5[38]. FBXL5 activity is regulated though iron and/or oxygen dependent prolyl hydroxylation[19,39]. Under iron deficient, or hypoxic conditions, FBXL5 fails to recognize IRP2, and thus IRP2 proteins levels are stabilized leading to increase IRP2 expression and IRP RNA binding activity. Conversely, iron excess enhances FBXL5 activity, resulting in IRP2 ubiquitination and proteasomal degradation[38,40].

Iron metabolism in cancer cells:

Cancer cells require more iron to maintain their rapid and endless proliferation and growth rates. Iron is essential for DNA synthesis, and it also generates free radicals which contribute to gene mutation and may hasten tumor initiation [3]. Indeed, distinct iron related gene

expression patterns are associated with both the development of metastases and patient survival[15,41,42]. For example, TFRC is highly expressed in many cancer cells such as breast, prostate, and colorectal cancer, which would be predicted to promote tumor growth by increasing iron uptake and availability [43-45]. One of the mechanisms contributing to increased TFRC expression in cancer is transcriptional activation via the oncogene, c-Myc, which is one of the most frequently dysregulated proteins in human cancer. Intriguingly, TFRC has been shown to activate expression of c-Myc[46]. Thus, therapeutically targeting TFRC may have significant value as TFRC knockout has been shown to decrease cellular proliferation in many cancer types[47-49] .

Normally, excess iron will be stored in ferritin to prevent the generation of reactive oxygen species (ROS). The role of ferritin in cancer development has shown to be tumor specific where changes in ferritin levels may halt or promote tumorigenesis[46,50,51]. For instance, in breast cancers cells with an aggressive mesenchymal phenotype, such as MDA-MB-231 cells, it was shown that elevated ferritin expression was associated with tumor growth[50]. Meanwhile, knockdown of ferritin halted the proliferation and tumorsphere formation in cancer stem-like cells[51]. Nonetheless, cancer cells also have an altered iron export thus different types of cancer display altered regulation of ferritin.

IRP signaling can also be corrupted in cancer, presumably in an effort to acquire sufficient iron to support rapid cell proliferation. For example, IRP2 overexpression in breast cancer results in increased TFRC expression, decreased FTH expression, and subsequently an increase iron labile pool and worse cancer prognosis[52]. Intriguingly however, IRP1 overexpression was actually found to decrease tumor growth in vivo[53]. Thus, despite their similar roles in the maintenance of iron homeostasis, IRP1 and IRP2 exhibit opposing

phenotypes in the reduction and promotion of tumor growth, respectively. Therefore, continued investigation into the roles that IRPs play in cancer progression is warranted.

Epithelial-to-mesenchymal transition:

The epithelial-to-mesenchymal transition (EMT) is a temporary and reversible biological cellular event that naturally occurs in a broad range of tissues. EMT is critical for the early developmental stage and wound healing, but it can also become activated during pathologic conditions such as cancer, ischemia, and chronic inflammation[7,8,54,55]. During EMT, epithelial cells are progressively altered to resemble a mesenchymal-like cell where profound biological differences are present. Epithelial cells tend to be non-motile, polarized, and embedded via cell-cell tight junction in cell colonies, but during EMT they dissolve their cell-cell junctions and convert into individual, non-polarized, motile, and highly invasive mesenchymal cells[56]. EMT is thought to occur largely through changes in gene expression. Specially for genes whose downstream targets are important for the epithelial state such as adherent junction components (e.g., E-Cadherin) and tight junction components (e.g., tight junction protein 1), and such genes are repressed by EMT transcription factors including Snail Family Transcriptional Repressor 1 (SNAI1), Twist Family BHLH Transcription Factor 1 (TWIST), and transforming growth factor-β 1 (TGFβ1)[6,10]. At the same time, the cells also express genes associated with a mesenchymal state by shifting the expression of cadherin and intermediate filaments.

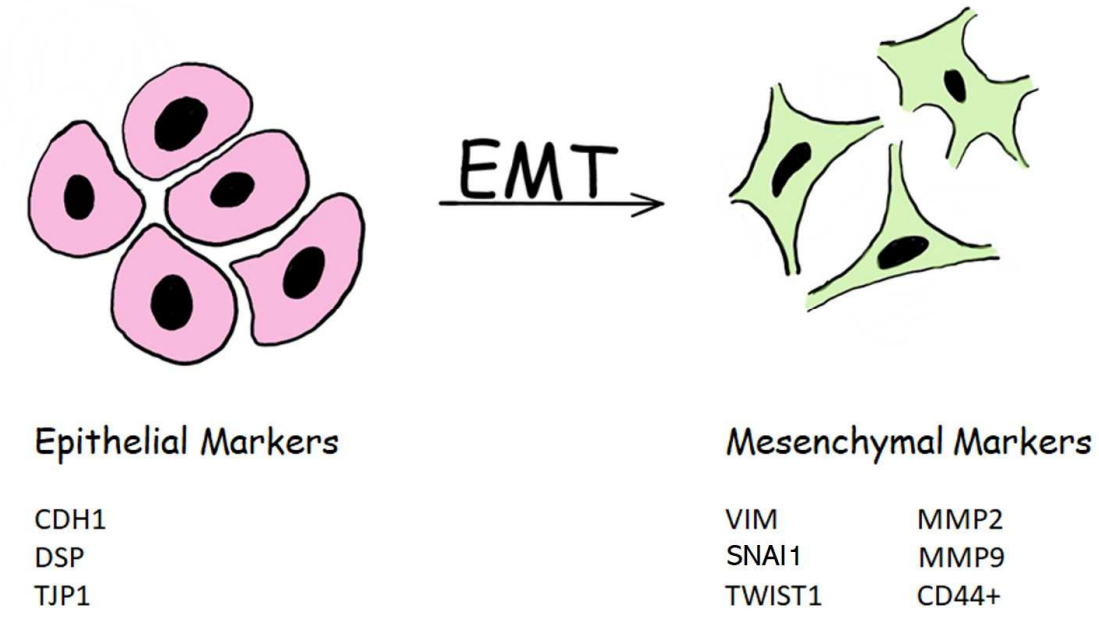

Figure 1. Genes commonly expressed in the epithelial to mesenchymal transition. E-Cadherin (CDH1), desmoplakin (DSP), tight junction protein (ZO-1) are expressed in epithelial cells. Vimentin (VIM), SNAI1 (Snail Family Transcriptional Repressor 1), Twist Family BHLH Transcription Factor 1 (TWIST1), matrix metalloproteinases (MMP-2 and MMP-9), and cluster of differentials 44 (CD44+) are expressed in mesenchymal like cells.

The cytoskeleton, composed of the actin filaments, microtubules, and intermediate filaments provide structural design and mechanical strength that is necessary to mold cell shape. Although these cytoskeleton components act concurrently, the actin filaments are the main driving force of cell migration by reorganizing its structure[57]. The microtubule network also undergoes modifications during EMT that leads to the formation of microtentacles, a microtube-based membrane extension, at the invasive side[57,58]. Intermediate Filaments, ubiquitous in eukaryotic cells, are the most rubbery and insoluble structures in cells with the function of supporting the plasma membrane and maintain cell shape[57]. This family of protein has six isoforms, of which vimentin (VIM) and nestin attract the most attention. During EMT process, intermediate filaments are typically rearranged from cytokeratin-rich to vimentin-rich networks as a result motility capacity is significantly enhanced[59,60].

The loss of cell-cell adhesion and the acquisition of a cytoskeletal architecture that confers mobility and invasiveness that occurs during EMT is believed to be a key driver of tumor metastasis. As such, understanding, the mechanisms that facilitate EMT could lead to the developmental of improved cancer therapies. Recent studies in the cancer biology field have identified iron as an important regulator of EMT process by demonstrating that mesenchymal-like cancer stem cells have an increased dependence in intracellular[61]. Yet, the mechanisms promoting mesenchymal iron acquisition and utilization are not understood.

In addition to the change of morphology EMT also drives an increase in matrix metalloproteinases (MMPs) expression. As the name may suggest, MMPs are enzymes responsible for degrading extracellular matrix (ECM) such as collagen, gelatin, stromelysins, and

others thus facilitating cellular invasion as well as detachment of epithelial cells from surrounding tissues[62].

Ferroptosis: An iron mediated form of cell death

Cell death is important for normal development, homeostasis, and the prevention of hyperproliferative diseases such as cancer. It was once thought that this essential tool in the cell's arsenal was regulated mostly by the activation of caspases that resulted in apoptosis[63,64]. Dixon et. al observed that a drug called erastin caused cell death that could not be halted by apoptotic inhibitors and did not share morphological characteristics with apoptotic, necrotic, or autophagy driven cell death. In addition, it was shown that adding iron chelators, such as desferrioxamine (DFO), and antioxidants, such as and ferrostatin (Fer-1) prevented ferroptotic cell death. Thus, the term ferroptosis was adopted to describe this distinct form of regulated cell death that is characterized by lethal, iron-dependent accumulation of peroxidized lipids[33,65,66].

The mechanism by which erastin induced ferroptosis was found to be via the inhibition of system x_c^-. The system x_c^- mediates the exchange of extracellular l-cysteine and intracellular l-glutamate necessary for the synthesis of GSH. Without GSH synthesis of glutathione peroxidase (GPX4), the major phospholipid hydroperoxide neutralizing enzyme, is impaired leading to toxic lethal levels of ROS[65,67]. Thus, any perturbations of the cell's natural ability to produce glutathione and protect against oxidative stress can enhance susceptibility to ferroptotic cell death[68].

Since its identification in 2012, ferroptosis was found to be involved the pathophysiology of neurological diseases, ischemic organ damage, and cardiovascular diseases[67,69]. Inhibitors of

ferroptosis have been shown to prevent tissue damage in models of ischemia/reperfusion and hemochromatosis and to be protective in models of degenerative brain disorders such as Parkinson's, Huntington's, and Alzheimer's disease[70-72]. On the other hand, ferroptosis inducers show promise in cancer therapy. For example, mesenchymal-like, cancer-stem cells, and the so-called "therapy-persister" cells are often resistant to apoptosis and common oncogenic therapies but are susceptible to ferroptosis due it elevated ROS load[12,67,68,73,74].

The epigenetically plastic SW13 cells: A model for EMT

The 2D cell culture model is widely used among the scientific community due its affordability, reproducibly, simplicity, and ease to interpret results among many others[75]. Although it isn't an equivalent replicate of the environment in organisms, this method is a good approach to first investigate a biological event without the complexities of an *in vivo* system. Here we use the human adrenal cortical carcinoma SW13 cell line as a prime research model for studying EMT as it exists as two distinct phenotypes that are epigenetically plastic[13,14,76].

In cell culture, about 2% of SW13 cells exist as a slow growing, highly invasive, mesenchymal-like subtype designated as SW13+, whereas the more abundant SW13- subtype is a rapidly growing, epithelial-like cell type, with diminished migratory properties[13,14]. While the SW13 subtypes were initially characterized by dilution cloning, it was later shown that SW13- cells can be converted to the SW13+ phenotype with the use of histone deacetylase inhibitors (HDACi)[13,14]. This unique feature allows us to temporally control EMT initiation, and thus affords us with a powerful model for investigating the alterations in iron homeostasis during both EMT initiation and progression. In this study, we utilize the SW13 cell line as a model of

epigenetic phenotype regulation to examine how alterations in iron availability influence HDAC inhibitor-mediated EMT and ferroptosis sensitivity.

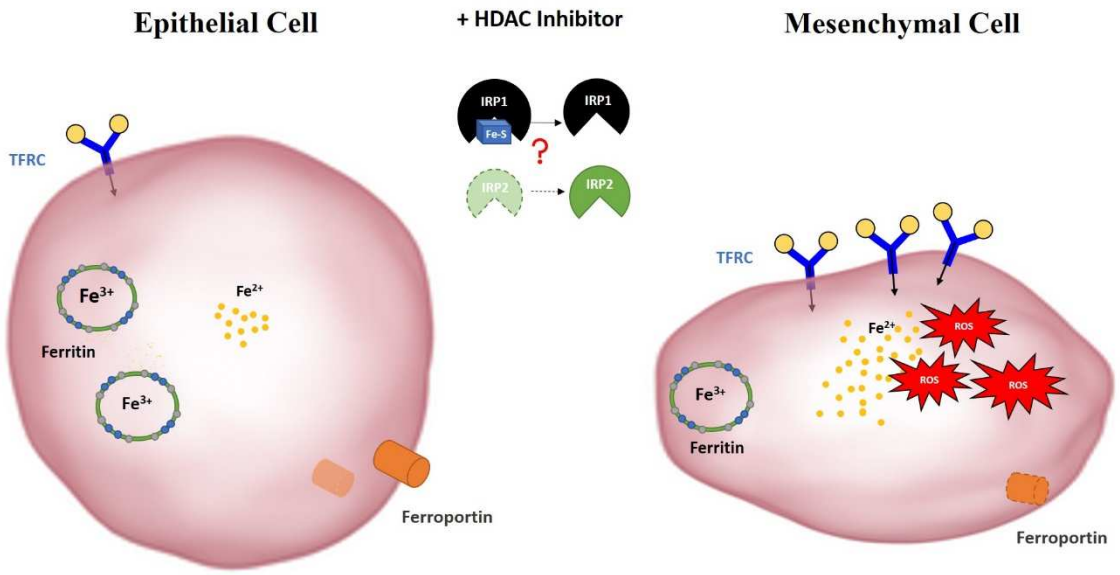

Figure 2. Working model for IRP-mediated iron accumulation during the epithelial to mesenchymal transition in SW13 cells. Following HDAC inhibitor treatment, SW13- cells undergo a phenotypic transition that includes reduced cellular proliferation, the acquisition of metastatic traits, and the accumulation of intracellular iron. We hypothesize that intracellular iron accumulation is mediated by increased IRP mRNA binding activity, leading to increased iron uptake by TFRC while storage of iron in ferritin and export of iron by ferroportin is decreased. Consequently, the size of the labile iron pool and reactive oxygen species (ROS) production is increased.

CHAPTER III

METHODOLOGY

Cell Culture

The SW13 cell line (ATCC CCL-105) is a primary small cell adrenal gland/cortex carcinoma cell line derived from a 55-year-old Caucasian human. For all experiments, cells were grown in (37ºC, 95% humidity, 5% CO2) DMEM 1640 1X with L-glutamine (Corning #17-207-CV Manassas, VA) supplemented with 10% fetal bovine serum and 1% penicillin streptomycin 100X (Corning #30-002-Cl Manassas, VA).

Cell Treatment:

For EMT induction, SW13 cells lines were treated with 2 nM Romidepsin (Fk228, Selleckchem, #93020) for 48 hours. To examine the influence of iron availability on EMT, SW13 cells were treated with 2 nM FK228 for 24 hours and co-treated with 50 μM or 25 μM of the iron chelator, desferrioxamine (DFO) or 40 μM the iron containing porphyrin, hemin 24 h, respectively for 24 hours. All experiments followed the describe treatment dose and length unless mentioned otherwise in the methods session.

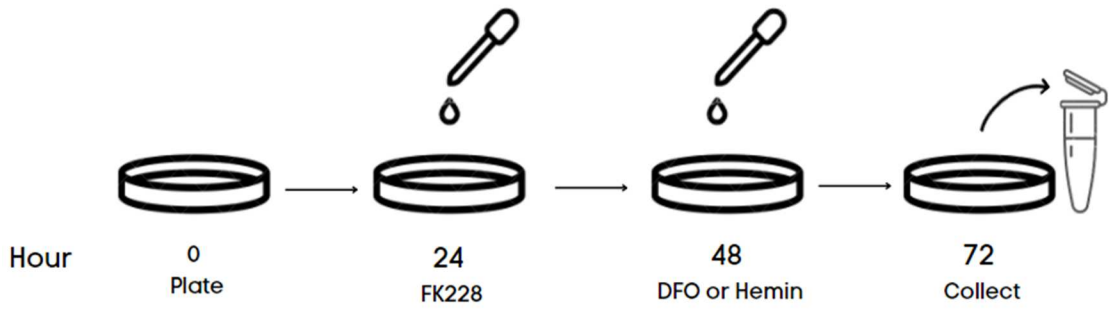

Figure 3. Illustration of the treatment timeline. Cells were incubated with FK228 for 48 h as this length of treatment has previously been shown to induce EMT[13,14]. Iron supplementation or chelation was induced by treating cells with hemin or DFO for 24 h.

Western blot

Western blot was used to measure markers of iron metabolism at the protein level. Total protein was harvested from the SW13+ subtype by removing the adherent cells with cell stripper creating a cell suspension with the saved media. The collected cell suspension was then be centrifuged at 1,000 x *g* for 5 minutes at 4ºC. The cells were then be washed with 1X PBS and re-pelleted at 1,000 x *g* for 5 minutes at 4ºC. Cells were lysed with RIPA buffer (50 mM Tris-HCl, pH 8.0, 1% NP-40, 0.5% Na-deoxycholate, 0.1% SDS, 2 mM EDTA, 150 mM NaCl, Halt Protease inhibitor cocktail (ThermoFisher), 1 mM DTT, 1mM Citrate, 1mM phenylmethylsulphonyl fluoride (PMSF), 10µM Mg132). Samples were vortexed every 5 minutes for 20 minutes followed by centrifugation at 14,000 x *g* for 15 minutes at 4ºC. The supernatant was collected and stored at -80ºC. Total protein concentration was determined based on the bicinchoninic acid assay (Thermo Fisher Scientific, Waltham, MA, Cat #23209). Thirty micrograms total protein in a RIPA and 2 X Laemmli sample buffer (0.01% Bromophenol blue, 4% SDS, 10% 2-mercaptoethanol, 20% glycerol, 0.125 M Tris-HCl pH 6.8) were heated at 95ºC for 5 minutes to denature the proteins then loaded into a Mini-PROTEAN TGX Stain-Free Precast gel with 4-20% polyacrylamide (Biorad # Hercules, CA) and electrophoresed at 150V for 60 minutes and then be transferred onto a PVDF membrane at 300 mA for 75 minutes. Equal transfer was confirmed with Ponceau S staining before blocking of the membrane for 1 hour in 5% nonfat milk in 1X TBS-Tween at room temperature. Blots were incubated in CD71/TFRC (Cell signaling, #D7S5Z), SLC40A1 (ferroportin; FPN) (Invitrogen, #PA5-22993), and GAPDH (Santa Cruz, #0411) primary antibody overnight at 4ºC at 1:1000 dilution in 5% non-fat dry milk in 1X Tris-buffered saline with 0.01% Tween-20. HRP-linked secondary antibodies were used at

1:10,000 dilution for 1 h at room temperature to detect primary antibody biding. The blot was then washed before being imaged with chemiluminescence (ProteinSimple Fluorchem, R&D Systems) and analyzed using ImageJ software[77]

Immunofluorescence

To assess changes in morphology immunofluorescence was performed using standard techniques. SW13 cells were fixed with 4 % paraformaldehyde, permeabilized with 0.2 % Triton-X, and blocked with 1 % BSA before incubation with 1:1000 Alexafluor 488 (Invitrogen, A12379) in 1%BSA 1X PBS for 1 h in the dark. Three washes were performed with 1X PBS prior mounting coverslip with DAPI. Samples were photographed using a Keyence BZ-X700 Fluorescent Microscope at $495_{excitation}/518_{emission}$ and $360_{excitation}/460_{emission}$ for actin filaments and DAPI, respectively, with uniform exposure.

CellRox

CellRox deep red (#C10422; Thermofisher) was used to measure oxidative stress following FK228 treatment. Cells were seeded into pre-collagen coated 8-well chamber slides (Ibidi, #80841) at 10,000 cells/well and treated with 2nM FK228 for 48 hours. Cells were washed once with Hank's Balanced Salt Solution (HBSS)(Cellgro, 21-022-CV) prior incubation with CellRox reagent at a final concentration of 5uM for 30 min at 37 ^{o}C. Then, the cells were washed twice with HBSS, and the fixed with 4 % paraformaldehyde. Three washes of 1X PBS were performed prior mounting slide with DAPI. Samples were imaged at 40X using a Keyence BZ-X700 Fluorescent Microscope with fluorescence read at 640 $nm_{excitation}$/665 $nm_{emission}$ and 360

$nm_{excitation}$/460 $nm_{emission}$. Low photobleach settings and exposure were held consistent through imaging process.

Cell viability

Cells were seeded at 4000 cells per well in a 96 well plate and cultured for 24 h before treatment with DMSO (vehicle) or the previously described doses of FK228 and DFO or Hemin. Cell viability measured using PrestoBlue (ThemoFisher) according to the manufacturer's instruction. Fluorescence was read at $560_{excitation}$/$570_{emission}$ using Biotek Synergy H1 (Biotek, Winooski, VT, USA) plate reader. Differences in cell viability were normalized relative to the vehicle control group for each cell line.

Cell proliferation assay

To assess the impact of iron availability on proliferation of HDAC inhibitor induced EMT, cells were seeded into pre-collagen coated 8-well chamber slides (Ibidi, #80841) at 4000 cells/well. Cells were treated with FK228 and DFO or hemin as previously described and 10 μM Click-iT EdU reagent (ThermoFisher, #C10337) at the 48 hours' time mark. Prior imaging, nucleus was stained with Hoeschst 33342 stain 1:1000 (Thermofisher, #62249) for 10 min. Cells were then imaged at 4X live imaged using a Keyence BZ-X700 Fluorescent Microscope at 361 $nm_{excitation}$/497 $nm_{emission}$ and 495 $nm_{exictation}$/519 $nm_{emission}$ wavelengths for Hoechst and EdU, respectively. Low photobleach settings and exposure were held consistent through imaging process. ImageJ software[77] was used to count numbers of green (EdU) and blue (Hoechst) nucleus and percent proliferation was determined by the ratio between number of newly synthesized DNA (EdU) by the total nuclei (Hoechst).

Intracellular iron measurements

Total intracellular iron was measured in SW13 and H1299 cell lines following FK228 treatment for 48 h. At least 1 x 10^6 cells were counted prior lysed, and total intracellular iron levels were determined by measuring its colorimetric reaction with an Iron Assay Kit (MilliporeSigma; MAK025-1KT). Total intracellular iron levels were normalized to picogram per cell.

RNA Extraction

To determine gene expression changes in each cell line following FK228 treatment, cells were seeded in a 6-well plate at 3 x 10^5 cell/well and allowed to grow for 24 hours before treatment with 2 nM FK228. After the 48-hour treatment, media was aspirated from the wells and cells were homogenized using 800 µl of Trizol (Invitrogen Cat# 15596026), collected into microcentrifuge tubes and incubated for 5 minutes. Then 160 µl of chloroform were added and the samples were incubated for 3 minutes before being centrifuged at 12,000 x *g* for 15 minutes. at 4ºC. The supernatant was transferred to a fresh microcentrifuge tubes and 400 µl of 100% isopropanol was added to each tube. Samples were stored at -80 ºC overnight to increase RNA precipitation and yield. The next day, the samples were centrifuged at 12,000 x *g* for 15 minutes at 4ºC. The supernatant was then removed and the RNA pellet was washed in RNase-free 75% ethanol, vortexed and recollected by centrifugation at 7500 x *g* for 5 minutes at 4ºC. Samples were then dried and re-suspended in nuclease free water. Concentration, OD260/230 and OD260/280 ratios of RNA were measured using a Nanodrop (Thermo Fisher Scientific) spectrometer to check for purity of samples. RNA integrity was assessed by electrophoresis on a 1 % agarose 1% bleach gel at 100V for 30 minutes. Samples were stored at -80ºC.

Real Time Quantitative Polymerase Chain Reaction (RT-QPCR)

For RT-qPCR, 1 µg total RNA was used to create cDNA. For cDNA synthesis, 1 µg RNA, was DNase treated and then reverse transcribed using Superscript II (Thermo Fisher Scientific). Each reaction contained SYBR green chemistry, 50 ng cDNA, and 2.5 µM of the primer mix obtained from Integrated DNA technology (IDT, Coraville, IA). Reactions were performed on an ABI 7900HT Real-Time PCR system (ThermoFisher; Waltham, MA, USA) and mRNA expression levels were analyzed using relative quantification $2^{-\Delta\Delta Ct}$ method and Cq values were obtained for the genes measure. The sequences for the housekeeping gene (CYCLO) and genes of interested analyzed are listed in **Table 2.**

Gene	Forward	Reverse
CYCLO	5’tgccatcgccaaggagtag	5’tgcacagacggtcactcaaa
TFRC	5'agttgaacaaagtggcacgagcag	5'agcagttggctgttgtacctctca
FPN	5'tgaccagggcgggaga	5’agaggtcaggtagtcggcca
HMOX1	5’cgggccagcaacaaagtg	5’gtgtaaggacccatcggagaa
VIM	5’gctcgtcaccttcgtgaata	5’tcgttgataacctgtccatctc
TGFβ1	5’tcctggcgatacctcagcaa	5’ctcattttcccctccacggc
SNAI1	5’gctgcaggactctaatccaga	5’atctccggaggtgggatg
BRM	5’gattgtagaagacatccattgtgg	5’gacatataaccttggctgtgttga
SLC7A11	5’atgcagtggcagtgaccttt	5’ggcaacaaagatcggaactg
GPX4	5’acaagaacggctgcgtggtgaa	5’gccacacacttgtggagctaga
ACSL-4	5’agaatacctggactgggaccgaag	5’tgctggactggtcagagactgtaa

Table 2. Primer sequences for qPCR

Electrophoretic Mobility Shift Assay (EMSA)

In order to analyze spontaneous IRP IRE biding activity, SW13 cells were treated with 2 nM FK228 for 24 hours and total protein was harvested by removing the adherent cells with cell stripper creating a cell suspension with the saved media. The collected cell suspension was then centrifuged at 1,000 x *g* for 5 minutes at 4ºC. The cells were washed with 1X PBS and re-pelleted at 1,000 x *g* for 5 minutes at 4ºC. Then, the cell pellet was re-suspended in 2-volumes cytosol buffer (1mM HEPES, 10mM KCl, 0.1 mM EGTA, 0.1 mM EDTA, 1 mM DTT, 0.1M PMSF, 10 µM Mg132, 100 X Halt protease inhibitor cocktail (ThermoFisher). After 15 minutes, 0.1 volume of 10% NP40 was added to the suspension and the samples were vortexed for 10 seconds then centrifuged at 12,000 x *g* for 10 minutes at 4 C. Then, supernatant (cytosol) was removed to a fresh microfuge tube and stored at -80º C until use. Cytosolic protein concentration was determined based on the bicinchoninic acid assay (ThermoFisher Scientific, #23209). Spontaneous IRP1 and IRP2 RNA binding activities was assessed by incubating 5 µg total protein with saturating levels of [^{32}P] labeled RNA from the L-ferritin IRE as previously described[78]. Total IRP1 RNA binding activity was measured by adding 1 µg of cytosolic protein in the presence of 4% β-mercaptoethanol to saturating levels of RNA.

<u>Statistical Analyses:</u>

Differences in cell growth, proliferation, viability, and lipid peroxidation were analyzed using one-way ANOVA. When statistically significant effects were identified by ANOVA, post hoc analyses were performed to make pairwise comparisons using the Tukey HSD method. Also, Student's t-test was used to compare differences between treatment group and control in total iron and relative mRNA expression. All tests were performed using SPSS v23.0 software (IBM-SPSS;

Chicago, IL, USA). Descriptive statistics were calculated for all variables and include mean ± SEM. All experiments were repeated 3 times, with n = 3 per group.

CHAPTER IV

FINDINGS

HDAC inhibitor treatment induces EMT and promotes iron accumulation in SW13 cells.

The epigenetically plastic SW13 cell line exists as two distinct subtypes whose switch can be epigenetically regulated[13,14]. The rapidly growing, highly tumorigenic, epithelial-like subtype SW13- accounts for majority of a SW13 colony, while the other subtype SW13+ is a slow growing, metastatic, and more mesenchymal-like that accounts to a small percentage of the total colony. It has been previously shown that HDAC inhibitors induce the phenotype transition from the tumorigenic SW13- to the metastatic SW13+, and the conversion can be confirmed by the expression of the tumor suppressor protein BRM[13]. Thus, we hypothesized that HDAC inhibitor treatment of SW13 cells could serve as uniquely powerful model that would allow us to temporally control EMT initiation. To confirm that the HDAC inhibitor-induced SW13 phenotype conversion indeed models canonical EMT signaling pathways, cells were treated with 2 nM FK228 for 48 hours, and morphology and EMT markers were assessed. **Figure 4A** shows the representative images of SW13 under control conditions (left panel) where cells displayed an epithelial-like cortical actin cytoskeleton. Whereas, HDAC inhibitor treatment (right panel) resulted in loss of cell-cell tight junctions and a mesenchymal-type morphology evidenced by their fiber-like actin organization. SW13+ phenotype conversion was further confirmed by the strong induction of BRM mRNA expression (Figure 4B). Such as large increase was observed

because, as expected, BRM mRNA expression in untreated SW13 cells was nearly undetectable. To support our hypothesis that the SW13 mesenchymal phenotype shift was occurring via an EMT-like process, we analyzed EMT gene expression markers by qPCR. Indeed, the relative mRNA expression of transforming growth factor-β 1 (TFG-β1) and SNAI1, which are critical for EMT induction, significantly increased 1.5-fold and 2.4 fold, respectively (**Figure 4C**). Recent studies in the cancer biology field have identified iron as an important regulator of EMT process by demonstrating that mesenchymal-like cancer stem cells have an increased dependence on intracellular iron[11,61], and so we also investigated the influence of SW13 phenotype conversion on total intracellular iron. HDAC inhibitor treatment significantly increased total intracellular iron levels by 29.5% in SW13 cells, $p < 0.05$. These findings indicate that SW13 cells can serve as a model for exploring the link between iron and EMT.

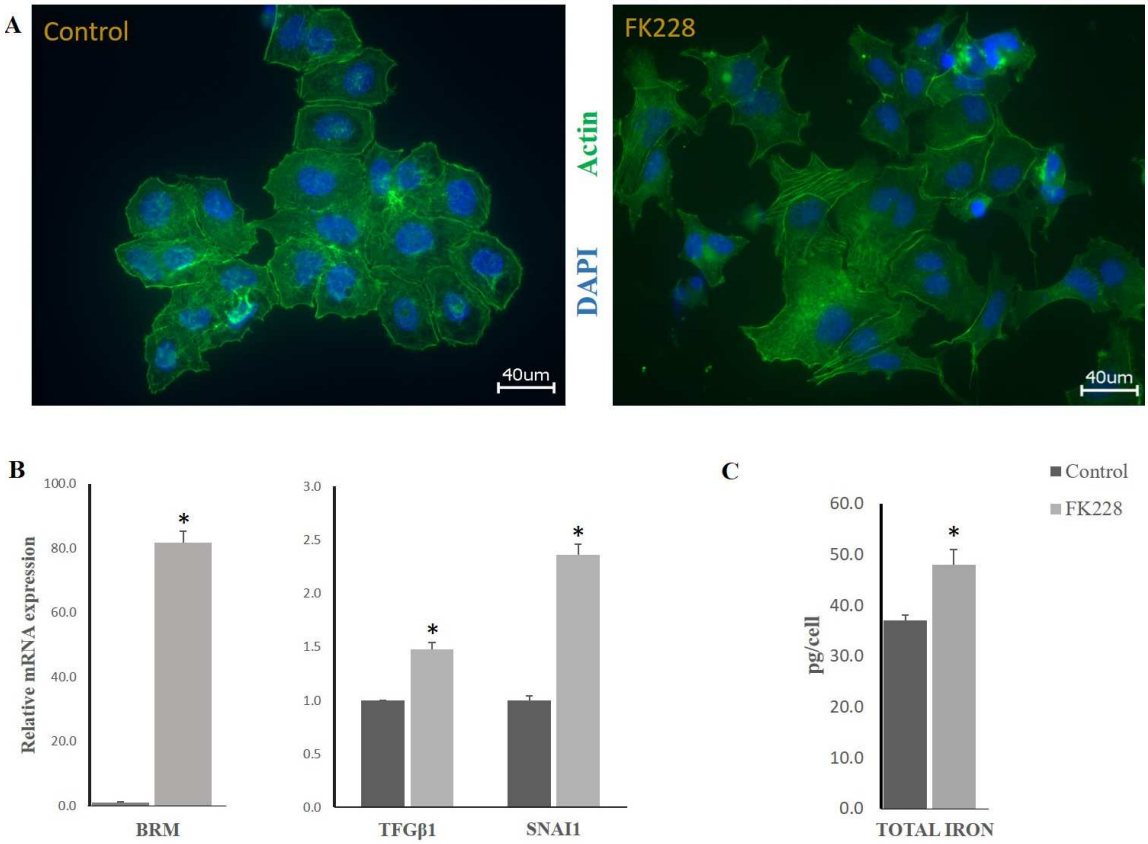

Figure 4. HDAC inhibitor induces-mediated SW13 phenotype conversion can serve as a model of the epithelial to mesenchymal transition. (**A**) Treatment with 2 nM FK228 alters SW13 cell morphology and actin (green) organization, induces the expression of (**B**) the mesenchymal markers BRAHMA (BRM), transforming growth factor 1 gene (TGFβ1), snail family transcriptional repressor 1 (SNAI1), and promotes (**C**) intracellular iron accumulation. Images were taken using a 40X objective lens. Data are presented as mean ± SEM. * Denotes significant difference compared to control, $p < 0.05$.

Iron availability does not interfere with SW13 cell phenotype conversion.

Iron chelation has previously been shown to attenuate TGFβ1-induced EMT[10]. Thus, we sought to determine how alterations in iron availability could influence HDAC inhibitor-induced EMT in SW13 cells. To do so, cells were treated with 2 nM FK228 for 24 hours, and then were treated with either 50 μM DFO or 40 μM hemin to assess how iron chelation or iron supplementation, respectively, influence changes in morphology and the expression of EMT markers. Intriguingly, a much smaller number of cells were observed following co-treatment with FK228 and DFO, and while some more fiber-like cortical actin structures were observed, several more epithelial-like clusters of cells were observed as well. Contrarily, the iron supplemented FK228 treated cells (bottom right-hand) appeared very similar to cells treated with FK228 alone.

As iron chelation appeared to have a more significant impact on HDAC inhibitor mediated EMT in SW13 cells, we then investigated the influence of DFO treatment on the expression of EMT markers. Cells were co-treated with FK228 and DFO as described above and the expression of BRM, TGFβ1, and SNAIL1 mRNA was measured by qPCR. These finding suggest, that at in SW13 cells, once EMT is initiated, limiting cellular iron availability Is not sufficient to block the EMT process.

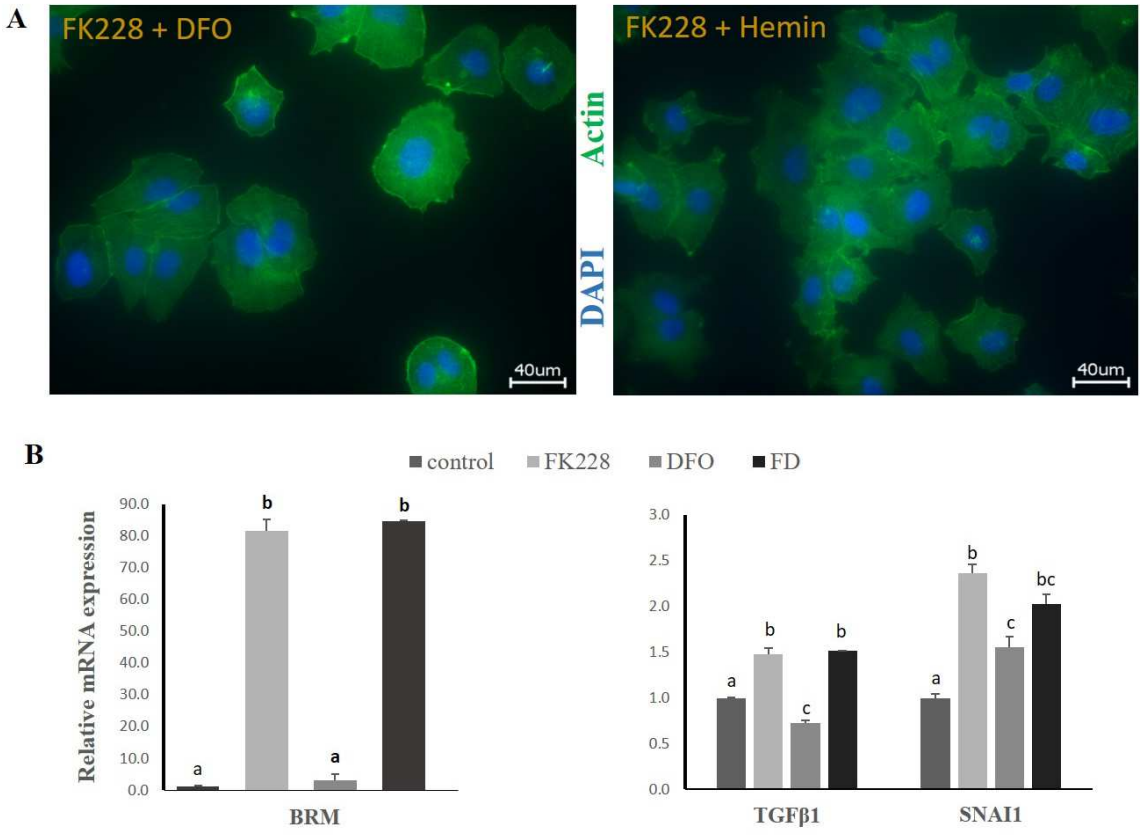

Figure 5. Changes in cellular iron availability does not alter HDAC inhibitor mediated EMT in SW13 cells. (**A**) Morphology differences following 2 nM FK228 treatment for 24 hours and then co-treatment with 50 μM DFO or 40 μM hemin for another 24 hours. (**B**) Co-treatment with DFO did not impact the FK228-mediated increase in the expression of the EMT markers BRM, TGFβ1, or SNAI1 in SW13 cells. Images were taken using a 40X objective lens. Data are presented as mean ± SEM. Superscript denotes statistical significance, $p < 0.05$. Treatments that share the same superscript are not statistically different.

Iron regulatory proteins contribute to iron accumulation during HDAC inhibitor-mediated SW13 cell EMT.

Intracellular iron homeostasis is regulated by iron regulatory proteins (IRP1 and IRP2). These proteins bind mRNA in an iron-dependent fashion, thereby "sensing" intracellular iron status and, accordingly, coordinating the uptake, storage, and utilization of iron. Thus, to investigate the mechanisms contributing to increased intracellular iron following SW13 cell EMT, we analyzed the activity of IRPs following HDAC inhibitor treatment. In SW13 cells, spontaneous IRP mRNA binding activity significantly increased 14%, from 57 ± 2 to 74 ± 3 fmol RNA/mg protein following 2 nM FK228 treatment for 24 hours, $p < 0.01$, **Figure 6B**.

The addition of the reductant β-Mercaptoeathanol (β-ME) results in disassembly of the Fe-S cluster in IRP1 and slight increase in the binding of the latent IRP2 thus allowing for the measurement of the total IRP1/2 protein present[79]. Following the addition of β-ME to the same cytoplasmic extracts from SW13 cells, we observed a significant increase in total IRP mRNA binding capacity ~14%, from 415 ± 20 to 525 ± 22 fmol/mg, $p < 0.02$, **Figure 5D**. These findings suggest that the observed increase is likely due to an increase in the total abundance of IRPs. Regardless of mechanism, increased IRP mRNA binding is expected to increase the expression of the iron uptake protein, TFRC, and decrease the expression of the iron export protein, ferroportin[18,19,27,78,79]. While we did not observe the expected corresponding increase in the expression of TFRC, ferroportin expression was decreased in SW13 cells following HDAC inhibitor treatment, **Figure 6E**. These finding suggests that the accumulation of iron in SW13 cells, as it transition to a mesenchymal phenotype, is a result from its lack of ability to export intracellular iron.

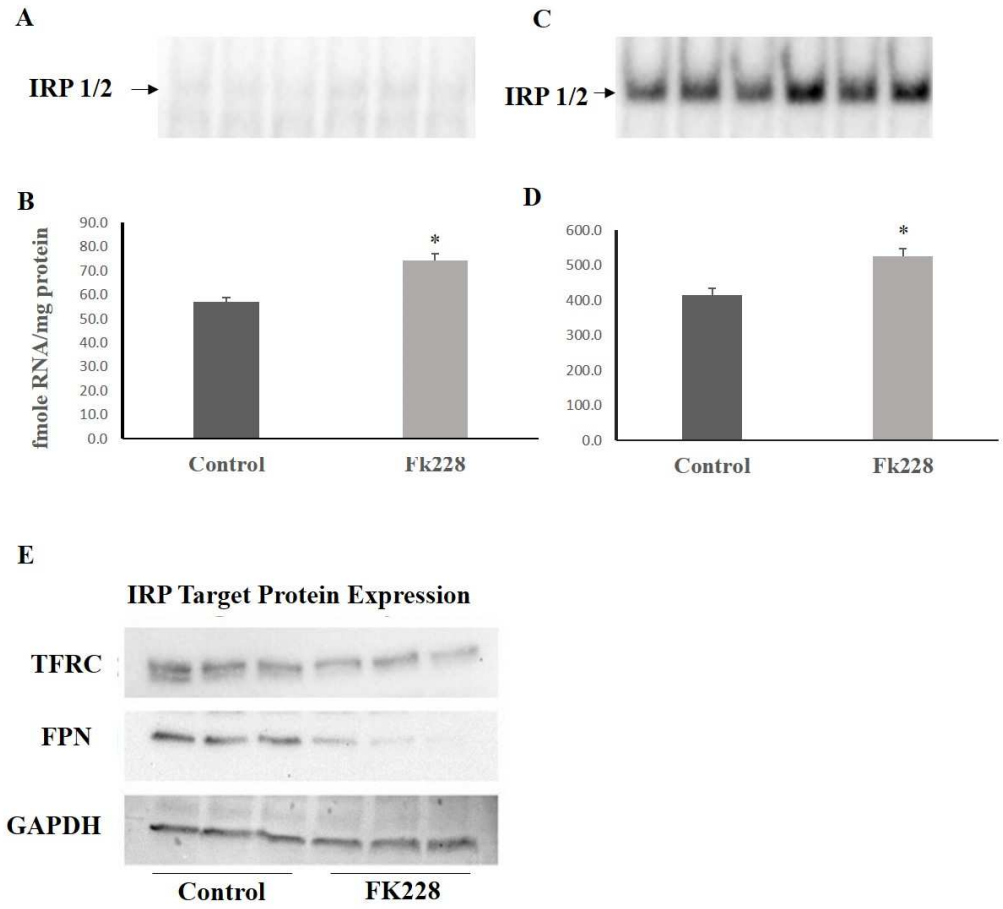

Figure 6. IRP mRNA binding activity is increased and ferroportin expression is decreased following HDAC inhibitor-mediated EMT in SW13 cells. **(A,B**) Spontaneous and (C,D) total IRP1/2 mRNA binding activity was assayed by gel shift in SW13 cell line following 5 nM FK228 treatment for 24 hours and quantitated revealing a significant increase in spontaneous IRP RNA binding. (**E)** Changes in protein expression of transferrin receptor (TFRC) and ferroportin (FPN), downstream targets of IRPs, results in decreased export of intracellular iron. * Denotes statistical differences from control, $p < 0.02$. Data are presented as mean ± SEM.

Iron chelation and iron supplementation can reduce proliferation and promote cell death in HDAC inhibitor treated SW13 cells.

HDAC inhibitors have been extensively studied for their anti-cancer properties[80-83]. However, while HDAC inhibitors induce toxicity and slow cell growth in some cell types, they can also increase metastatic properties and chemotherapy resistance in others[54,80,84]. As iron is also critical for tumor cell growth, we were interested whether manipulation of intracellular iron availability could improve HDAC inhibitor treatment outcomes. SW13 cell proliferation and viability was assessed following co-treatment with 2 nM FK228 and 50 μM DFO or 40 μM as described below, **Figure 7A**. As expected, proliferation was significantly reduced following FK228 treatment alone, $p < 0.05$. However, co-treatment with either DFO or hemin did not further decrease proliferation rates (**Figure 7B)**. To understand whether the observed decrease in proliferation was due to a slowdown in cell division or some toxic effect from iron chelation or iron overload, we next assessed cell viability. Viability was unaffected by FK228 treatment alone, but notably both iron chelation and iron supplementation in combination with FK228 treatment significantly decreased cell viability as indicated by a reduced number of metabolically active cells (**Figure 7C)**. Collectively, these results indicate that HDAC inhibitor-induced mesenchymal-like SW13 cells are more sensitive to alterations in iron availability and suggest that manipulation of iron-dependent pathways could be used to enhance the therapeutic efficacy of HDAC inhibitors.

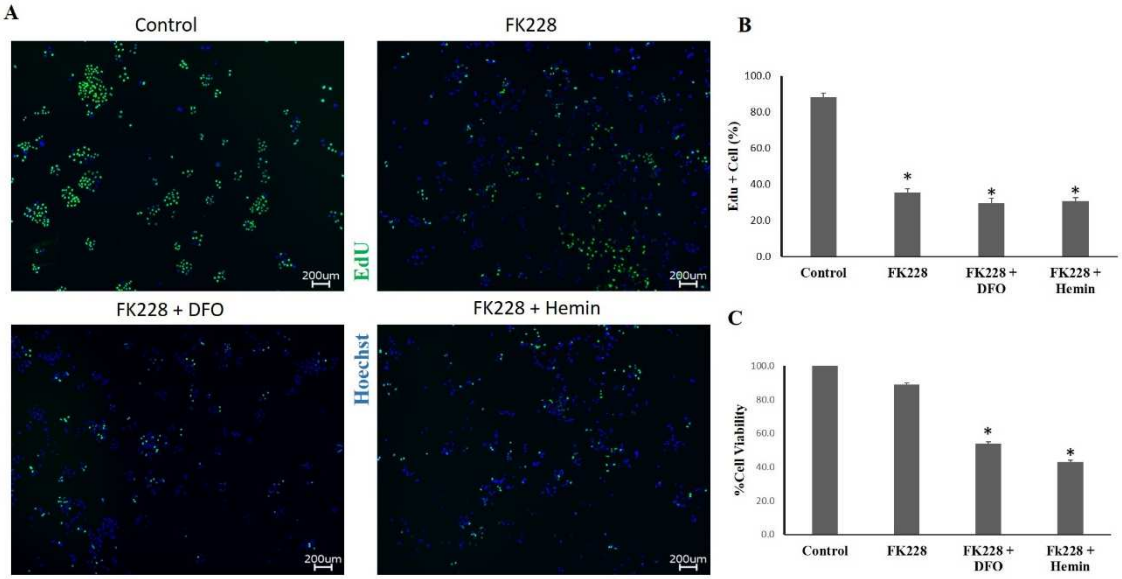

Figure 7. Both iron chelation and iron supplementation reduce cell viability in HDAC inhibitor treated SW13 cells. (**A**) Images and (B) quantitation of EdU-positive ratio in SW13 cells following 2 nM FK228 treatment for 24 hours and then co-treatment with 50 μM DFO or 40 μM hemin for another 24 hours (**C**) Percent cell viability was measured by fluorometric assay. Images were taken on 4X objective lens. * Denotes statistical significance, $p < 0.05$. Treatments with a shared superscript are not statistically significant. Data are presented as mean ± SEM.

SW13 cells exhibit increased oxidative stress during HDAC inhibitor mediated EMT.

Due to its propensity to form free radicals, iron is an essential but potentially toxic nutrient. To investigate mechanisms that could contribute to increased sensitivity to alterations in iron availability following HDAC inhibitor induced EMT in SW13 cells we used a fluorescent probe to measure cytosolic oxidative stress and found that SW13 cells have significantly higher levels of ROS following 48 hours of FK228 treatment (**Figure 8A)**. To further investigate other variables that may contribute to the observed increased oxidative stress, we analyzed the expression of genes involved in the antioxidant response[85]. Interestingly, HDAC inhibitor treatment significantly decreased the mRNA expression of glutathione peroxidase 4 (GPX4), superoxide dismutase 1 (SOD1), solute carrier family 7 member 11 (SLC7A11), and tumor suppressor superoxide dismutase 1 (SOD1), the solute carrier family 7 member 11 (SLC7A11), and the tumor suppressor TP53 (**Figure 8B**). As this gene signature is consistent with an induced ROS pattern that is often observed in ferroptosis, we also examined the mRNA expression of acyl-CoA synthase long-chain family member 4 (ACSL4), which is critical for the production of polyunsaturated fatty acids that are required for phospholipid peroxidation and ferroptosis[65,66,68]. Indeed, ACSL4 mRNA expression was also increased following HDAC inhibitor treatment (**Figure 8B**). Altogether, the weaken antioxidant defenses and increase in a lipogenic marker suggests that EMT induced SW13 cells may be more susceptible to ferroptosis, an iron mediated form of cell death.

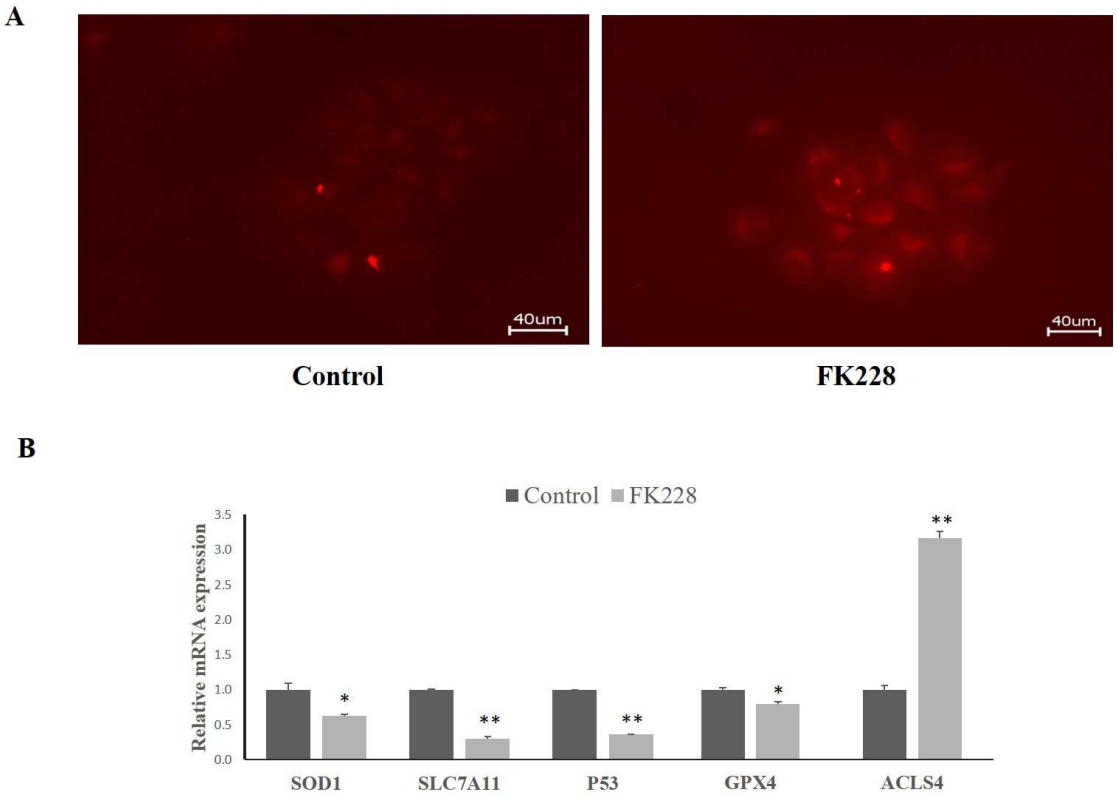

Figure 8. HDAC inhibitor-converted mesenchymal-like SW13 cells have increased levels of ROS and reduced expression of antioxidant defense genes. (**A**) SW13 cells exhibited increased oxidative stress following 2 nM FK228 treatment measure by incubating cells with 5 μM Cell Rox deep red reagent for 30 minutes prior images were taken on 40X objective lens. (**B**) The relative mRNA abundance of the antioxidant genes solute carrier (SLC7A11), tumor suppressor gene (TP53), glutathione peroxidase (GPX4), and superoxide dismutase (SOD1) significantly decreased, while mRNA abundance of the lipogenic gene, acyl-CoA synthase long-chain family member 4 (ACSL4), significantly increased. * Denotes significance when compared to control, $p < 0.001$. ** Denotes significance when compared to control, $p < 0.00005$. Data are presented as mean ± SEM.

HDAC inhibition enhances ferroptosis sensitivity in mesenchymal-like SW13 cells.

An ideal environment for ferroptosis to occur involves an increased labile iron pool (LIP) and a decrease of the natural antioxidant defenses of the cell. An abnormal LIP carries a danger for the cells as it can interact with phospholipids containing polyunsaturated fatty acids chains (PUFA-PLs) to generate ROS[65]. Thus, we hypothesized that HDAC inhibitor treatment would increase SW13 cell susceptibility to ferroptosis. To test this hypothesis, we assessed cell viability and lipid peroxidation following 24 and 48 hours of HDAC inhibitor treatment, with or without erastin (1 uM or 5 uM), a potent inducer of ferroptosis. At 24 hours, only the higher dose erastin treatment significantly reduced cell viability (**Figure 9A**), which was also observed at 48 hours (**Figure 9B**). However, after 48 hours, we also observed significantly more cell death in SW13 cells that were co-treated with FK228 and the low dose of erastin than when they were treated with erastin alone at an equivalent dose (**Figure 9B)**. Lethal lipid peroxidation is a hallmark of ferroptosis thus we used BODIPY C-11, a lipid peroxidation sensor, to measure ROS generated by lipids. BODIPY was performed for 24 and 48 hours with 5 μM Erastin and/or 2 nM FK228 treatment hours. Interestingly, at 24 hours FK228 alone exhibited the highest levels of lipid peroxidation among all groups, **Figure 9C**. On the other hand, at 48 hours 5 μM erastin alone displayed the highest levels of lipid peroxidation, **Figure 9D**. While timing appears to be an important factor to be taken in consideration, altogether the results suggest that ferroptosis may be a viable approach to improve therapeutic outcomes of HDAC inhibitor treatments.

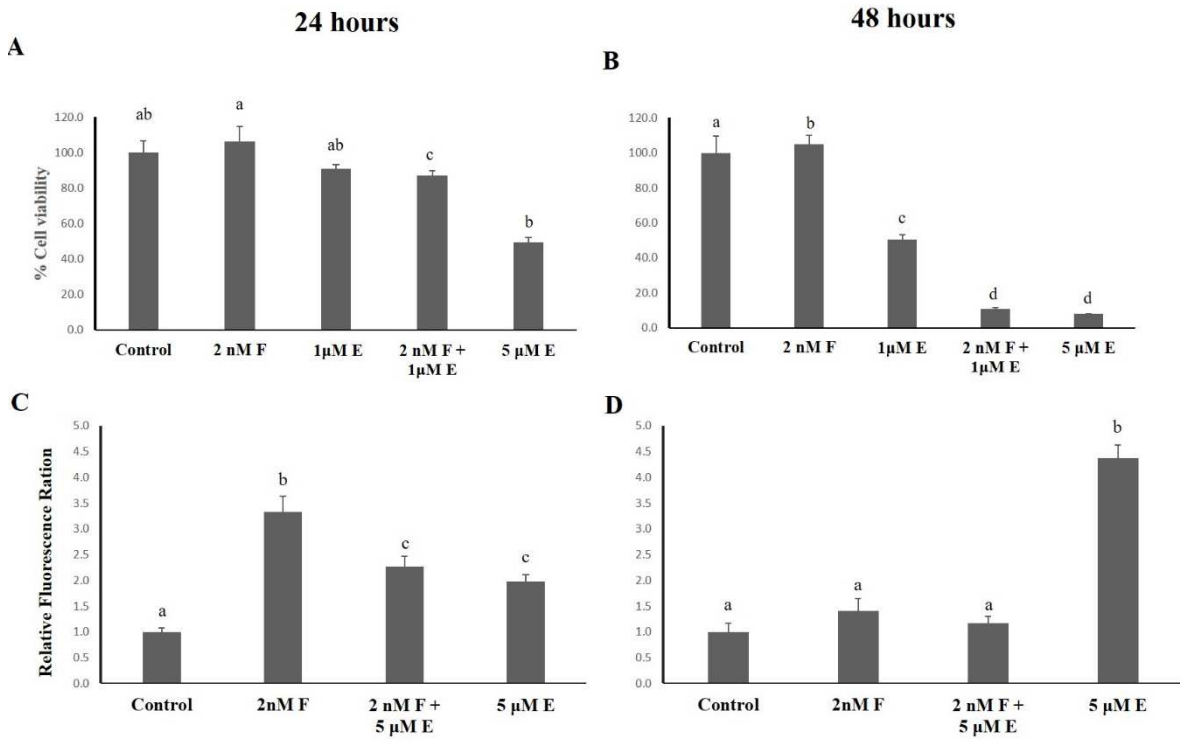

Figure 9. Ferroptosis induction synergistically improve HDAC inhibitor treatment on SW13 cells. Cell viability was assessed at 24 hours (**A**) and 48 hours (**B**) following treatment with the FK228 (1 nM or 2 nM) and/or erastin (1,3, or 5 μM). Lipid peroxidation was assayed using BODIPY C11 probe following 2 nM FK228 and/or 5 μM erastin for 24 (**C**) and 48 hours (**D**). Changes in viability and amounts of oxidized probe were quantified relative to the control. Superscript denotes statistical difference, $p < 0.05$. Treatment with a shared superscript it is not statistically significant. Data are presented as mean ± SEM.

CHAPTER V

DISCUSSION

The epithelial-to-mesenchymal transition is a normal event in living organisms occurring during embryonic development, tissue regeneration, and wound healing. However, EMT is also implicated in the pathogenesis of many disease as well, such as ischemia and reperfusion and numerous cancers. EMT is an undesirable for those with any type of cancer as it involved with tumor growth, metastatic expansion, and the generation of tumor cells with stem cell -like properties that play a major role in resistance to cancer treatments[6,7,58]. Intriguingly, adoption of a mesenchymal state is also associated with increased iron uptake[51,61,86] and enhanced sensitivity to ferroptosis[12], but the mechanisms promoting mesenchymal cell iron acquisition and utilization are not understood.

To begin to elucidate the link between iron adoption of a mesenchymal state, we utilized the SW13 cell line that can be driven through the EMT process by HDAC inhibitor treatment. First, we established that treatment with 2 nM FK228 for 48 hours was sufficient to induce morphologic changes consistent with EMT, and that these changes coincide with the increased expression of classical EMT-driving transcription factors, TFGβ1 and SNAI1[6,8,10]. Also, in agreement with previous findings, the more mesenchymal-like HDAC inhibitor treated SW13

cells were found to have higher levels of intracellular iron[51], establishing them as a model system for exploring the relationship between iron and EMT.

To investigate the mechanisms contributing to the accumulation of iron following EMT, we began by analyzed changes in IRP mRNA binding as IRPs the primarily regulators of intracellular iron homeostasis[18,20]. Interestingly, both spontaneous and total IRP mRNA binding increased about 14% each following HDAC inhibitor treatment. As human IRP1 and IRP2 do not separate during standard gel shift analyses we cannot determine the individual contributions to the increase in spontaneous and total IRP mRNA binding. However, as IRP1 is regulated by insertion and removal of an Fe-S cluster, whereas IRP2 is regulated at the level of protein stability, it is tempting to speculate that the equivalent increase in spontaneous IRP binding and total IRP protein levels are due to increased IRP2 stability alone. Future research should interrogate mechanisms that could promote IRP2 stability during HDAC inhibitor induced EMT.

To determine how increased IRP mRNA binding activity could contribute to the increased levels of intracellular iron in HDAC inhibitor converted mesenchymal-like SW13 cells, we next examined the expression of two downstream IRP targets, TFRC and ferroportin. Typically, an increase in IRP mRNA binding is results in the stabilization of mRNA containing 3'IRE such as TFRC and the inhibition of the translation of mRNA containing 5'IRE leading to increased iron uptake and reduced iron uptake, respectively[18,19]. While we did not observe the expected corresponding increase in the expression of the iron uptake protein, ferroportin protein expression was significantly reduced following HDAC inhibitor treatment. These findings are consistent with previous research demonstrating that suppression of ferroportin alone can promote EMT, presumably by increasing iron availability to the tumor[17,87]. Thus, exploration of

mechanisms that could restore ferroportin expression during EMT could potentially help limit tumor cell iron availability and mitigate tumor expansion. Currently, the question remains as to how and why IRP mRNA binding activity is increased in HDAC inhibitor-converted mesenchymal-like SW13+ cells even though cellular iron levels are higher.

In this regard, we questioned whether the apparent perturbation in IRP-dependent iron sensing during SW13 cell EMT could be exploited to improve HDAC inhibitor treatment outcomes. That is, could we harness the previously observed benefits of HDAC inhibitor-mediated reduced proliferation while mitigating undesirable consequences of increased invasiveness and chemotherapeutic resistance[13,14]. We found that while neither iron chelation nor iron supplementation further reduced proliferation in HDAC inhibitor treated cells, both treatments promoted increased cell death. While these findings are consistent with the essential, yet potentially toxic nature of iron, to develop successful iron-targeted therapeutic strategies, it is first necessary to understand how manipulation of iron availability can lead to augmented cell death in HDAC inhibitor treated cells.

Increased levels of intracellular iron, as observed in the mesenchymal-like SW13 cells, can contribute to the formation of ROS that can both drive EMT, but also damage the DNA of cells, ultimately leading to cell death[68]. Thus, we next examined how HDAC inhibitor mediated EMT influenced cellular ROS production and found that ROS levels were significantly higher following HDAC inhibitor treatment. To investigate factors that could be contributing higher ROS levels following HDAC inhibitor-mediated EMT, we measured the expression of genes involved in the antioxidant response and observed a significant reduction in antioxidant gene expression. EMT has also been shown to increase sensitivity to iron-mediated cell death by

promoting phospholipid peroxidation via the upregulation of ACSL4[68], and we observed a significant increase in ACSL4 expression as well. Altogether, the increased levels of intracellular iron, reduced antioxidative capacity, and enhanced lipid peroxidation signaling pathways indicated that induction of EMT in SW13 cells may increase their sensitivity to ferroptotic cell death.

To test this hypothesis, we treated cells with the potent ferroptosis inducer, erastin, either by itself or in combination with the HDAC inhibitor for 24 and 48 hours and measured changes in lipid peroxidation and cell viability. Intriguingly, increasing levels of lipid peroxidation did not correlate with reduced levels of cell viability. This could be a result of looking at static ROS levels at singular timepoints however, rather than total ROS production over the total treatment time periods. Importantly though, by 48 hours, significantly more cell death was observed in SW13 cells that were co-treated with FK228 and erastin then when they were treated with erastin alone at an equivalent dose. These results suggest that HDAC inhibitor-mediated EMT can enhance ferroptosis sensitivity and that HDAC inhibitor treatment could be used synergistically to augment ferroptotic cell death.

In this study, we have established the epigenetically plastic SW13 cell line as a model to temporally control EMT initiation and explore the relationship between iron and EMT[54,80,84]. Using this model, we have established the HDAC inhibitor-converted mesenchymal-like SW13 cells have increased intracellular iron accumulation, diminished IRP sensing of intracellular iron levels, and reduced antioxidative capabilities that significantly increase their susceptibility to ferroptotic cell death. The importance of these studies is underscored by the fact that iron is both an essential, yet potentially toxic nutrient. Thus, understanding how to manipulate iron

availability in specific cell types, while minimizing the impact on patient iron homeostasis are essential components to the development of iron-targeted therapeutic strategies. In this regard, ferroptosis is an ideal pathway to target as activation of ferroptosis can facilitate cell death by weakening the cell's antioxidant defenses against the free iron that is already inside the cell. Herein, we show that HDAC inhibitor treatment can augment ferroptosis sensitivity in SW13 cells by inducing EMT. The implications of these findings are significant as many other cell types have also been shown to adopt a mesenchymal phenotype following HDAC inhibitor treatment[54]. Moreover, as several HDAC inhibitors are already used clinically to treat a wide variety of diseases, the findings from these studies could be used to develop iron-targeted therapeutic strategies that will improve clinical outcomes for multiple disorders.

CHAPTER VI

CONCLUSION

Iron is an important nutrient that facilitates cell proliferation and growth. However, iron can be detrimental as it can phase between its reduced and oxidized form leading to free radical formation. An excess of free radicals contributes to DNA damage thus tumor initiation and progression[9,11]. The most aggressive types of cancer adopt a stem cell phenotype which is correlated with metastasis and chemotherapy resistance[6,58]. The switch from epithelial to mesenchymal phenotype is regulated by EMT transcription factors, that in turn, are upregulated by ROS. It has been observed that mesenchymal cancer cells have a higher dependency on iron, and that iron chelation reduces EMT makers by decreasing ROS formation[10,12]. The mechanisms of iron acquisition by mesenchymal cells are yet not be fully elucidated.

Histone deacetylases inhibitors have been extensively studied in cancer biology due its ability to alter the cell's epigenetic make-up. The success was limited to liquid cancers (e.g., T-lymphoma) however with little success on solid tumors[83]. The use of HDAC inhibitor promoted mesenchymal phenotypes several types of cancer including colon, prostate, and breast[54,80,88]. The epigenetically plastic adenocarcinoma SW13 was shown to convert from epithelial-to-mesenchymal phenotype by the use of HDAC inhibitor, and conversion could be confirmed by increased expressions of the BRM gene[13,14]. Thus, to hypothesize that HDAC inhibitor -induced

EMT SW13 cells can be used as a powerful model that allow us to temporarily initiate EMT. We did observe increase mesenchymal markers and morphology change in the HDAC inhibitor – induced SW13 cells.

In agreement with previous data, SW13 cells accumulated iron as they transitioned to a mesenchymal phenotype following HDAC inhibitor which led us to use this model to study the effects of iron availability on EMT outcomes. We found that neither iron chelation nor iron supplementation alter proliferation and mesenchymal markers of HDAC inhibitor. However, it did decreased viability thus showing the essential/toxic effects of iron. Yet, the mechanisms behind the observed accumulation of iron still needed to be explore. As expected, we saw an increase in IRP mRNA binding followed by a decreased ability to export iron. After investigating the potential side-effects of an increased LIP, we found that the HDAC inhibitor treated group exhibited an increase in ROS as well as a decrease in antioxidant properties. In addition, the generated ROS was derived in part from lipid peroxidation. A cell with increased LIP and lipid peroxidation, and reduced antioxidant capacity is a perfect environment to ferroptosis. Indeed, mesenchymal like SW13 cells were more sensible to ferroptotic cell death. Viswanathan et. al. also showed that mesenchymal cells were more susceptible to ferroptosis due its increased dependency on the GPX4 antioxidant pathway.

Our findings suggests that HDAC inhibitor induced EMT SW13 cells are a powerful model that could be extended to study other metabolites that may be involved during the EMT conversion. We also shown that mesenchymal SW13 cells have an increased dependency on iron as either iron chelation or supplementation affects cells viability. The accumulation of iron was due to a decreased ability of export iron. In addition, EMT induced SW13 cells display increase

oxidative stress and decreased antioxidant defense, scenario that can be taken advantage off. Although manipulation of iron appears an attractive approach to cancer therapy, its vitality for systemic processes makes it a challenge. Instead, targeting the elevated intracellular iron of mesenchymal cells might be a clearer approach as it is has a specific target. As the implication of these finding can be extended to other cell lines, these findings are relevant to a variety of clinically important cancer research and drug development.

REFERENCES

References:

1. Jung M, Mertens C, Tomat E, Brune B. Iron as a Central Player and Promising Target in Cancer Progression. *Int J Mol Sci.* 2019;20(2).
2. Kwok JC, Richardson DR. The iron metabolism of neoplastic cells: alterations that facilitate proliferation? *Critical Reviews in Oncology/Hematology.* 2002;42(1):65-78.
3. Zhou L, Zhao B, Zhang L, et al. Alterations in Cellular Iron Metabolism Provide More Therapeutic Opportunities for Cancer. *Int J Mol Sci.* 2018;19(5).
4. Choi JD, Lee J-S. Interplay between Epigenetics and Genetics in Cancer. *Genomics Inform.* 2013;11(4):164-173.
5. You JS, Jones PA. Cancer genetics and epigenetics: two sides of the same coin? *Cancer Cell.* 2012;22(1):9-20.
6. Aiello NM, Maddipati R, Norgard RJ, et al. EMT Subtype Influences Epithelial Plasticity and Mode of Cell Migration. *Dev Cell.* 2018;45(6):681-695 e684.
7. Lopez-Novoa JM, Nieto MA. Inflammation and EMT: an alliance towards organ fibrosis and cancer progression. *EMBO Mol Med.* 2009;1(6-7):303-314.
8. Zhang Y, Weinberg RA. Epithelial-to-mesenchymal transition in cancer: complexity and opportunities. *Front Med.* 2018;12(4):361-373.
9. Brown RAM, Richardson KL, Kabir TD, Trinder D, Ganss R, Leedman PJ. Altered Iron Metabolism and Impact in Cancer Biology, Metastasis, and Immunology. *Front Oncol.* 2020;10:476.
10. Chen Z, Zhang D, Yue F, Zheng M, Kovacevic Z, Richardson DR. The iron chelators Dp44mT and DFO inhibit TGF-beta-induced epithelial-mesenchymal transition via up-regulation of N-Myc downstream-regulated gene 1 (NDRG1). *J Biol Chem.* 2012;287(21):17016-17028.
11. El Hout M, Dos Santos L, Hamai A, Mehrpour M. A promising new approach to cancer therapy: Targeting iron metabolism in cancer stem cells. *Semin Cancer Biol.* 2018;53:125-138.
12. Viswanathan VS, Ryan MJ, Dhruv HD, et al. Dependency of a therapy-resistant state of cancer cells on a lipid peroxidase pathway. *Nature.* 2017;547(7664):453-457.

13. Davis MR, Daggett JJ, Pascual AS, et al. Epigenetically maintained SW13+ and SW13- subtypes have different oncogenic potential and convert with HDAC1 inhibition. *BMC Cancer.* 2016;16:316.
14. Montgomery MR, Hull EE. Alterations in the glycome after HDAC inhibition impact oncogenic potential in epigenetically plastic SW13 cells. *BMC Cancer.* 2019;19(1):79.
15. Lee HJ, Lee EK, Lee KJ, Hong SW, Yoon Y, Kim JS. Ectopic expression of neutrophil gelatinase-associated lipocalin suppresses the invasion and liver metastasis of colon cancer cells. *International Journal of Cancer.* 2006;118(10):2490-2497.
16. Wenners AS, Mehta K, Loibl S, et al. Neutrophil gelatinase-associated lipocalin (NGAL) predicts response to neoadjuvant chemotherapy and clinical outcome in primary human breast cancer. *PloS one.* 2012;7(10):e45826-e45826.
17. Pinnix ZK, Miller LD, Wang W, et al. Ferroportin and iron regulation in breast cancer progression and prognosis. *Sci Transl Med.* 2010;2(43):43ra56-43ra56.
18. Hentze MW, Muckenthaler MU, Galy B, Camaschella C. Two to tango: regulation of Mammalian iron metabolism. *Cell.* 2010;142(1):24-38.
19. Anderson CP, Shen M, Eisenstein RS, Leibold EA. Mammalian iron metabolism and its control by iron regulatory proteins. *Biochim Biophys Acta.* 2012;1823(9):1468-1483.
20. Stefania Recalcati GM, and Gaetano Cairo. Iron Regulatory Proteins: From Molecular Mechanisms to Drug Development. *Antioxidants & Redox Signaling.* 2010;13(10):1593-1616.
21. Conway D, Henderson MA. Iron metabolism. *Anaesthesia & Intensive Care Medicine.* 2019;20(3):175-177.
22. Donovan A, Lima CA, Pinkus JL, et al. The iron exporter ferroportin/Slc40a1 is essential for iron homeostasis. *Cell Metab.* 2005;1(3):191-200.
23. Hiromi G, Bryan M, Urs VB, et al. Cloning and characterization of a mammalian proton-coupled metal-ion transporter. *Nature.* 1997;388(6641):482.
24. Levi S, Luzzago A, Cesareni G, et al. Mechanism of ferritin iron uptake: activity of the H-chain and deletion mapping of the ferro-oxidase site. A study of iron uptake and ferro-oxidase activity of human liver, recombinant H-chain ferritins, and of two H-chain deletion mutants. *The Journal of biological chemistry.* 1988;263(34):18086.
25. Li JY, Paragas N, Ned RM, et al. Scara5 is a ferritin receptor mediating non-transferrin iron delivery. *Dev Cell.* 2009;16(1):35-46.
26. Li L, Fang CJ, Ryan JC, et al. Binding and uptake of H-ferritin are mediated by human transferrin receptor-1. *Proc Natl Acad Sci U S A.* 2010;107(8):3505-3510.
27. Wachnowsky C, Fidai I, Cowan JA. Iron-sulfur cluster biosynthesis and trafficking - impact on human disease conditions. *Metallomics.* 2018;10(1):9-29.

28. Fuss JO, Tsai CL, Ishida JP, Tainer JA. Emerging critical roles of Fe-S clusters in DNA replication and repair. *Biochim Biophys Acta.* 2015;1853(6):1253-1271.
29. Das D, Patra S, Bridwell-Rabb J, Barondeau DP. Mechanism of frataxin "bypass" in human iron-sulfur cluster biosynthesis with implications for Friedreich's ataxia. *J Biol Chem.* 2019;294(23):9276-9284.
30. Ye H, Rouault TA. Erythropoiesis and iron sulfur cluster biogenesis. *Adv Hematol.* 2010;2010.
31. Hunt JR, Zito CA, Johnson LK. Body iron excretion by healthy men and women. *Am J Clin Nutr.* 2009;89(6):1792-1798.
32. Piccinelli P, Samuelsson T. Evolution of the iron-responsive element. *RNA.* 2007;13(7):952-966.
33. Cao JY, Poddar A, Magtanong L, et al. A Genome-wide Haploid Genetic Screen Identifies Regulators of Glutathione Abundance and Ferroptosis Sensitivity. *Cell Reports.* 2019;26(6):1544-1556.e1548.
34. Beinert H, Kennedy M, Stout C. Aconitase as iron-sulfur protein, enzyme, and iron-regulatory protein. *Chemical Reviews.* 1996;96(7):2335.
35. Bouton C, Drapier J-C. Iron regulatory proteins as NO signal transducers. *Science's STKE : signal transduction knowledge environment.* 2003;2003(182):pe17.
36. Stys A, Galy B, Starzynski RR, et al. Iron regulatory protein 1 outcompetes iron regulatory protein 2 in regulating cellular iron homeostasis in response to nitric oxide. *J Biol Chem.* 2011;286(26):22846-22854.
37. Kim S, Ponka P. Role of nitric oxide in cellular iron metabolism. *Biometals.* 2003;16(1):125-135.
38. Salahudeen A, Thompson J, Ruiz J, et al. An E3 Ligase Possessing an Iron-Responsive Hemerythrin Domain Is a Regulator of Iron Homeostasis. *Science (Washington).* 2009;326(5953):722-726.
39. Guo B, Phillips JD, Yu Y, Leibold EA. Iron regulates the intracellular degradation of iron regulatory protein 2 by the proteasome. *The Journal of biological chemistry.* 1995;270(37):21645.
40. Moroishi T, Nishiyama M, Takeda Y, Iwai K, Nakayama KI. The FBXL5-IRP2 axis is integral to control of iron metabolism in vivo. *Cell Metab.* 2011;14(3):339-351.
41. Miller LD, Coffman LG, Chou JW, et al. An iron regulatory gene signature predicts outcome in breast cancer. *Cancer research.* 2011;71(21):6728.
42. Wenners AS, Mehta K, Loibl S, et al. Neutrophil Gelatinase-Associated Lipocalin (NGAL) Predicts Response to Neoadjuvant Chemotherapy and Clinical Outcome in Primary Human Breast Cancer (NGAL in Primary Human Breast Cancer). 2012;7(10):e45826.

43. Bogdan AR, Miyazawa M, Hashimoto K, Tsuji Y. Regulators of Iron Homeostasis: New Players in Metabolism, Cell Death, and Disease. *Trends Biochem Sci.* 2016;41(3):274-286.
44. Marques O, Porto G, Rêma A, et al. Local iron homeostasis in the breast ductal carcinoma microenvironment. *BMC Cancer.* 2016;16:187-187.
45. Radulescu S, Brookes Matthew J, Salgueiro P, et al. Luminal Iron Levels Govern Intestinal Tumorigenesis after Apc Loss In Vivo. *Cell Reports.* 2012;2(2):270-282.
46. Wu K-J, Polack A, Dalla-Favera R. Coordinated Regulation of Iron-Controlling Genes, H-Ferritin and IRP2, by c-MYC. *Science.* 1999;283(5402):676.
47. O'Donnell KA, Yu D, Zeller KI, et al. Activation of transferrin receptor 1 by c-Myc enhances cellular proliferation and tumorigenesis. *Mol Cell Biol.* 2006;26(6):2373-2386.
48. Aya S, Atsushi BT, Hitomi S, et al. Evaluation of Efficacy of Radioimmunotherapy with 90Y-Labeled Fully Human Anti-Transferrin Receptor Monoclonal Antibody in Pancreatic Cancer Mouse Models. *PLoS ONE.* 2015;10(4):e0123761.
49. Maffettone C, Chen G, Drozdov I, Ouzounis C, Pantopoulos K. Tumorigenic Properties of Iron Regulatory Protein 2 (IRP2) Mediated by Its Specific 73-Amino Acids Insert (A Role of IRP2 in Tumor Growth). *PLoS ONE.* 2010;5(4):e10163.
50. Shpyleva SI, Tryndyak VP, Kovalchuk O, et al. Role of ferritin alterations in human breast cancer cells. *Breast Cancer Res Treat.* 2011;126(1):63-71.
51. Schonberg DL, Miller TE, Wu Q, et al. Preferential Iron Trafficking Characterizes Glioblastoma Stem-like Cells. *Cancer Cell.* 2015;28(4):441-455.
52. Wang W, Deng Z, Hatcher H, et al. IRP2 regulates breast tumor growth. *Cancer Res.* 2014;74(2):497-507.
53. Chen G, Fillebeen C, Wang J, Pantopoulos K. Overexpression of iron regulatory protein 1 suppresses growth of tumor xenografts. *Carcinogenesis.* 2007;28(4):785-791.
54. Kong D, Ahmad A, Bao B, Li Y, Banerjee S, Sarkar FH. Histone deacetylase inhibitors induce epithelial-to-mesenchymal transition in prostate cancer cells. *PLoS One.* 2012;7(9):e45045.
55. Masola V, Zaza G, Gambaro G, et al. Heparanase: A Potential New Factor Involved in the Renal Epithelial Mesenchymal Transition (EMT) Induced by Ischemia/Reperfusion (I/R) Injury. *PLoS One.* 2016;11(7):e0160074.
56. Yilmaz M, Christofori G. EMT, the cytoskeleton, and cancer cell invasion. *Cancer Metastasis Rev.* 2009;28(1-2):15-33.
57. Sun BO, Fang Y, Li Z, Chen Z, Xiang J. Role of cellular cytoskeleton in epithelial-mesenchymal transition process during cancer progression. *Biomed Rep.* 2015;3(5):603-610.

58. Charpentier M, Martin S. Interplay of Stem Cell Characteristics, EMT, and Microtentacles in Circulating Breast Tumor Cells. *Cancers (Basel).* 2013;5(4):1545-1565.
59. Kim S, Coulombe PA. Intermediate filament scaffolds fulfill mechanical, organizational, and signaling functions in the cytoplasm. *Genes Dev.* 2007;21(13):1581-1597.
60. Nieminen M, Henttinen T, Merinen M, Marttila-Ichihara F, Eriksson JE, Jalkanen S. Vimentin function in lymphocyte adhesion and transcellular migration. *Nat Cell Biol.* 2006;8(2):156-162.
61. Mai TT, Hamai A, Hienzsch A, et al. Salinomycin kills cancer stem cells by sequestering iron in lysosomes. *Nat Chem.* 2017;9(10):1025-1033.
62. Radisky ES, Radisky DC. Matrix metalloproteinase-induced epithelial-mesenchymal transition in breast cancer. *J Mammary Gland Biol Neoplasia.* 2010;15(2):201-212.
63. Fuchs Y, Steller H. Programmed cell death in animal development and disease. *Cell.* 2011;147(4):742-758.
64. Solary E, Dubrez L, Eymin B. The role of apoptosis in the pathogenesis and treatment of diseases. *Eur Respir J.* 1996;9(6):1293-1305.
65. Cao JY, Dixon SJ. Mechanisms of ferroptosis. *Cell Mol Life Sci.* 2016;73(11-12):2195-2209.
66. Dixon SJ, Lemberg KM, Lamprecht MR, et al. Ferroptosis: an iron-dependent form of nonapoptotic cell death. *Cell.* 2012;149(5):1060-1072.
67. Li J, Cao F, Yin HL, et al. Ferroptosis: past, present and future. *Cell Death Dis.* 2020;11(2):88.
68. Jiang X, Stockwell BR, Conrad M. Ferroptosis: mechanisms, biology and role in disease. *Nat Rev Mol Cell Biol.* 2021;22(4):266-282.
69. Castellani RJ, Moreira PI, Liu G, et al. Iron: the Redox-active center of oxidative stress in Alzheimer disease. *Neurochem Res.* 2007;32(10):1640-1645.
70. Linkermann A, Skouta R, Himmerkus N, et al. Synchronized renal tubular cell death involves ferroptosis. *Proceedings of the National Academy of Sciences.* 2014;111(47):16836.
71. Skouta R, Dixon SJ, Wang J, et al. Ferrostatins inhibit oxidative lipid damage and cell death in diverse disease models. *J Am Chem Soc.* 2014;136(12):4551-4556.
72. Yagoda N, von Rechenberg M, Zaganjor E, et al. RAS-RAF-MEK-dependent oxidative cell death involving voltage-dependent anion channels. *Nature.* 2007;447(7146):864-868.
73. Liang C, Zhang X, Yang M, Dong X. Recent Progress in Ferroptosis Inducers for Cancer Therapy. *Adv Mater.* 2019;31(51):e1904197.

74. Hangauer MJ, Viswanathan VS, Ryan MJ, et al. Drug-tolerant persister cancer cells are vulnerable to GPX4 inhibition. *Nature.* 2017;551(7679):247-250.
75. Kapalczynska M, Kolenda T, Przybyla W, et al. 2D and 3D cell cultures - a comparison of different types of cancer cell cultures. *Arch Med Sci.* 2018;14(4):910-919.
76. Yamamichi-Nishina M, Ito T, Mizutani T, Yamamichi N, Watanabe H, Iba H. SW13 cells can transition between two distinct subtypes by switching expression of BRG1 and Brm genes at the post-transcriptional level. *J Biol Chem.* 2003;278(9):7422-7430.
77. Schneider CA, Rasband WS, Eliceiri KW. NIH Image to ImageJ: 25 years of image analysis. *Nature methods.* 2012;9(7):671-675.
78. Davis MR, Shawron KM, Rendina E, et al. Hypoxia inducible factor-2 α is translationally repressed in response to dietary iron deficiency in Sprague-Dawley rats. *J Nutr.* 2011;141(9):1590-1596.
79. Clarke SL, Thompson LR, Dandekar E, Srinivasan A, Montgomery MR. Distinct TP53 Mutation Subtypes Differentially Influence Cellular Iron Metabolism. *Nutrients.* 2019;11(9).
80. Ji M, Lee EJ, Kim KB, et al. HDAC inhibitors induce epithelial-mesenchymal transition in colon carcinoma cells. *Oncol Rep.* 2015;33(5):2299-2308.
81. Li D, Marchenko ND, Moll UM. SAHA shows preferential cytotoxicity in mutant p53 cancer cells by destabilizing mutant p53 through inhibition of the HDAC6-Hsp90 chaperone axis. *Cell Death and Differentiation.* 2011;18(12):1904.
82. Yan W, Liu S, Xu E, et al. Histone deacetylase inhibitors suppress mutant p53 transcription via histone deacetylase 8. *Oncogene.* 2013;32(5):599-609.
83. Yoon S, Eom GH. HDAC and HDAC Inhibitor: From Cancer to Cardiovascular Diseases. *Chonnam Med J.* 2016;52(1):1-11.
84. Lin K-T, Wang Y-W, Chen C-T, Ho C-M, Su W-H, Jou Y-S. HDAC inhibitors augmented cell migration and metastasis through induction of PKCs leading to identification of low toxicity modalities for combination cancer therapy. *Clinical cancer research : an official journal of the American Association for Cancer Research.* 2012;18(17):4691.
85. Birben E, Sahiner UM, Sackesen C, Erzurum S, Kalayci O. Oxidative stress and antioxidant defense. *World Allergy Organ J.* 2012;5(1):9-19.
86. Rychtarcikova Z, Lettlova S, Tomkova V, et al. Tumor-initiating cells of breast and prostate origin show alterations in the expression of genes related to iron metabolism. *Oncotarget.* 2017;8(4):6376-6398.
87. Shan Z, Wei Z, Shaikh ZA. Suppression of ferroportin expression by cadmium stimulates proliferation, EMT, and migration in triple-negative breast cancer cells. *Toxicol Appl Pharmacol.* 2018;356:36-43.

88. Zhu X, Huang S, Zeng L, et al. HMOX-1 inhibits TGF-β-induced epithelial-mesenchymal transition in the MCF-7 breast cancer cell line. *Int J Mol Med.* 2017;40(2):411-417.

VITA

THAIS GAIA OLIVEIRA

Candidate for the Degree of

Master of Science

Thesis: THE INFLUENCE OF HDAC INHIBITION ON THE MAINTAINANCE OF IRON HOMEOSTASIS AND THE AQUICSITION OF ONCOGENIC PHENOTYPES IN CANCER CELLS

Major Field: Nutrition Science and Dietetics

Biographical:

Education:

Completed the requirements for the Master of Science in Nutritional Science and Dietetics at Oklahoma State University, Stillwater, Oklahoma in December, 2021

Completed the requirements for the Bachelor of Science in Nutrition Science and Bachelor of Arts in Chemistry at East Carolina University, Greenville, North Carolina in May 2019.

Experience: Former Student Athlete

Professional Memberships:
Oklahoma Academy of Nutrition and Dietetics (OKAND)
North Central District Dietetic Association (NCDDA)
Academy of Nutrition and Dietetics